Design optimization of composite structures operating in acoustic environments

D. Chronopoulos[a]

[a]*Institute for Aerospace Technology, The University of Nottingham, NG7 2RD, UK*

Abstract

The optimal mechanical and geometric characteristics for layered composite structures subject to vibroacoustic excitations are derived. A Finite Element description coupled to Periodic Structure Theory is employed for the considered layered panel. Structures of arbitrary anisotropy as well as geometric complexity can thus be modelled by the presented approach. Damping can also be incorporated in the calculations. Initially, a numerical continuum-discrete approach for computing the sensitivity of the acoustic wave characteristics propagating within the modelled periodic composite structure is exhibited. The first and second order sensitivities of the acoustic transmission coefficient expressed within a Statistical Energy Analysis context are subsequently derived as a function of the computed acoustic wave characteristics. Having formulated the gradient vector as well as the Hessian matrix, the optimal mechanical and geometric characteristics satisfying the considered mass, stiffness and vibroacoustic performance criteria are sought by employing Newton's optimization method.

Keywords: Structural design optimization, Vibroacoustic response, Composite structures, Wave propagation

[Table 1 about here.]

1. Introduction

Layered and complex structures are nowadays widely used within the aerospace, automotive, construction and energy sectors with a general increase tendency, mainly because of their high stiffness-to-mass ratio and the fact that their mechanical characteristics can be designed to suit the particular purposes. Unluckily however, this high stiffness-to-mass ratio being responsible for the increased mechanical efficiency, at the same time induces high acoustic transmission through the structure. The need for simultaneously optimising an industrial structure of minimum mass and maximum static stiffness, while attaining satisfactory dynamic response performance levels is a challenging task for the modern engineer; especially when considering acoustic transmission through a layered structure which depends on the mechanical and geometric characteristics of each individual layer, resulting in a great number of design parameters to be optimised.

The numerical analysis of wave propagation within periodic structures was firstly considered in [1], while the work was extended to two dimensional media in [2]. The so called Wave Finite Element (WFE) method was introduced in

[3, 4] in order to facilitate the post-processing of the eigenproblem solutions and further improve the computational efficiency of the method. The interest in predicting the vibroacoustic response of a structure in a wave context is far from being new with the pioneering works of the authors in [5, 6, 7, 8] being probably the earliest ones. A layer-wise model for the prediction of acoustic wave propagation within continuous layered structures was presented in [9]. More recently, the prediction of the acoustic wave characteristics based on FE formulations allowed for more complex structures to be included in the acoustic transmission computations [10, 11, 12].

Structural sensitivity analysis is of great importance for understanding the overall impact of a design parameter variation to the performance characteristics which are to be optimised. Accurate sensitivity models are an important tool for design optimization, system identification as well as for statistical mechanics analysis. Several authors [13, 14, 15, 16] have been focusing on the eigenvalue derivative analysis of a structural system. With regard to the variability analysis of the waves travelling within a structural medium, the available published work is mainly focused on deriving expressions [17, 18] of the stochastic wave parameters from analytical models. In [19] the authors conduct a design sensitivity analysis by a wave based approach. Considering numerical approaches, the authors in [20] used Bloch's theorem in conjunction with the FE method in order to calculate the sensitivity of the acoustic waves within an auxetic honeycomb, while with regard to the computation of the variability of the propagating waves, the authors in [21, 22] have presented a stochastic WFE approach for computing the variability of wave propagation properties in one dimensional media. With regard to optimising the design characteristics of a layered structure the developed approaches have generally focused on genetic algorithms or particle swarm type techniques [23, 24, 25]. When it comes to optimising the structural design vis-a-vis the dynamic response performance of a structure, wave based optimization techniques have been developed [26, 27, 28, 29] by adopting Periodic Structure Theory (PST) assumptions.

In this work an established wave based SEA approach is employed in order to predict the vibroacoustic performance of a composite layered panel. The novelty of the work focuses on the derivation of the first and second order sensitivity of the acoustic transmission coefficient expressed through SEA with respect to the structural design characteristics of the modelled structure. The considered design parameters include the entirety of the mechanical characteristics, the density as well as the thickness of each individual structural layer. Non conservative structural systems are also modelled by the exhibited approach. Employing a three dimensional FE description of the modelled structure allows for capturing the entirety of the sound transmitting propagating structural waves, while employing a PST formulation allows for drastically reducing the computational cost related to calculating the SEA parameters and the Hessian matrix for each configuration. Although not discussed in this work, the method is straightforward to apply to curved structures by expressing the FE structural matrices and wave propagation properties in polar coordinates.

The paper is organized as follows: In Sec.2 the formulation of the sensitivity of the waves propagating within the periodic structure is elaborated. The PST to be employed is exhibited and the parametric sensitivity of the propagating waves with regard to the design of the modelled composite panel is deduced. Both conservative and non-conservative structural systems are considered. In Sec.3 the SEA model for computing the vibroacoustic performance of the layered panel is presented and its parametric sensitivity with respect to each design parameter of the panel is also derived.

The principal SEA quantities, namely the modal density, the radiation efficiency and the intrinsic damping loss factor are all considered. Once the parametric sensitivity of the vibroacoustic performance of the structure is computed, the formulation of the optimization problem, including the objective function as well as the corresponding Hessian matrix are formulated in Sec.4. In Sec.5 the presented approach is applied to a layered sandwich asymmetric structure and the corresponding numerical results are discussed. Conclusions on the presented work are eventually given in Sec.6.

2. Acoustic wave sensitivity

2.1. Formulation of the PST for an arbitrary structural segment

A periodic segment of a panel having arbitrary layering is hereby considered (see Fig.1) with L_x, L_y its dimensions in the x and y directions respectively. The segment is modelled using a conventional FE software. The mass, damping and stiffness matrices of the segment $\mathbb{M}$, $\mathbb{C}$ and $\mathbb{K}$ are extracted and the DoF set $\mathbf{q}$ is reordered according to a predefined sequence such as:

$$\mathbf{q} = \{\mathbf{q_I} \ \mathbf{q_B} \ \mathbf{q_T} \ \mathbf{q_L} \ \mathbf{q_R} \ \mathbf{q_{LB}} \ \mathbf{q_{RB}} \ \mathbf{q_{LT}} \ \mathbf{q_{RT}}\}^\top \tag{1}$$

corresponding to the internal, the interface edge and the interface corner DoF (see Fig.1). The free harmonic vibration equation of motion for the modelled segment is written as:

$$[\mathbb{K} + i\omega\mathbb{C} - \omega^2\mathbb{M}]\mathbf{q} = \mathbf{0} \tag{2}$$

[Figure 1 about here.]

The analysis then follows as in [10] with the following relations being assumed for the displacement DoF under the passage of a time-harmonic wave:

$$\mathbf{q_R} = e^{-i\varepsilon_x}\mathbf{q_L}, \quad \mathbf{q_T} = e^{-i\varepsilon_y}\mathbf{q_B}$$
$$\mathbf{q_{RB}} = e^{-i\varepsilon_x}\mathbf{q_{LB}}, \quad \mathbf{q_{LT}} = e^{-i\varepsilon_y}\mathbf{q_{LB}}, \quad \mathbf{q_{RT}} = e^{-i\varepsilon_x - i\varepsilon_y}\mathbf{q_{LB}} \tag{3}$$

with ε_x and ε_y the propagation constants in the x and y directions related to the phase difference between the sets of DoF. The wavenumbers k_x, k_y are directly related to the propagation constants through the relation:

$$\varepsilon_x = k_x L_x, \quad \varepsilon_y = k_y L_y \tag{4}$$

Considering Eq.3 in tensorial form gives:

$$\mathbf{q} = \begin{bmatrix} \mathbf{I} & \mathbf{0} & \mathbf{0} & \mathbf{0} \\ \mathbf{0} & \mathbf{I} & \mathbf{0} & \mathbf{0} \\ \mathbf{0} & \mathbf{I}e^{-i\varepsilon_y} & \mathbf{0} & \mathbf{0} \\ \mathbf{0} & \mathbf{0} & \mathbf{I} & \mathbf{0} \\ \mathbf{0} & \mathbf{0} & \mathbf{I}e^{-i\varepsilon_x} & \mathbf{0} \\ \mathbf{0} & \mathbf{0} & \mathbf{0} & \mathbf{I} \\ \mathbf{0} & \mathbf{0} & \mathbf{0} & \mathbf{I}e^{-i\varepsilon_x} \\ \mathbf{0} & \mathbf{0} & \mathbf{0} & \mathbf{I}e^{-i\varepsilon_y} \\ \mathbf{0} & \mathbf{0} & \mathbf{0} & \mathbf{I}e^{-i\varepsilon_x-i\varepsilon_y} \end{bmatrix} \mathbf{x} = \mathbf{Rx} \qquad (5)$$

with $\mathbf{x}$ the reduced set of DoF: $\mathbf{x} = \{\mathbf{q_I} \ \mathbf{q_B} \ \mathbf{q_L} \ \mathbf{q_{LB}}\}^\top$. The equation of free harmonic vibration of the modelled segment can now be written as:

$$[\mathbf{R}^*\mathbb{K}\mathbf{R} + i\omega\mathbf{R}^*\mathbb{C}\mathbf{R} - \omega^2\mathbf{R}^*\mathbb{M}\mathbf{R}]\mathbf{x} = \mathbf{0} \qquad (6)$$

with * denoting the Hermitian transpose. The most practical procedure for extracting the wave propagation characteristics of the segment from Eq.6 is injecting a set of assumed propagation constants ε_x, ε_y. The set of these constants can be chosen in relation to the direction of propagation towards which the wavenumbers are to be sought and according to the desired resolution of the wavenumber curves. Eq.6 is then transformed into a standard eigenvalue problem and can be solved for the eigenvector $\mathbf{x}$ which describe the deformation of the segment under the passage of each wave type at an angular frequency equal to the square root of the corresponding eigenvalue $\lambda = \omega^2$. It is noted that the computed angular frequency quantities $\omega = \omega_r + i\omega_i$ will have $|\omega_i| > 0$ implying complex values for the wavenumbers of the propagating wave types, otherwise interpreted as spatially decaying motion and from which the loss factor of each computed wave type w can directly be determined.

A complete description of each passing wave including its x and y directional wavenumbers and its wave shape for a certain frequency is therefore acquired. It is noted that the periodicity condition is defined modulo 2π, therefore solving Eq.6 with a set of ε_x, ε_y varying from 0 to 2π will suffice for capturing the entirety of the structural waves. Further considerations on reducing the computational expense of the problem are discussed in [10]. It should be noted that only propagating waves will be considered in the subsequent analysis.

2.2. Parametric sensitivity

2.2.1. Non conservative structural system

It is initially noted that matrices $\mathbf{K} = \mathbf{R}^*\mathbb{K}\mathbf{R}$, $\mathbf{C} = \mathbf{R}^*\mathbb{C}\mathbf{R}$ and $\mathbf{M} = \mathbf{R}^*\mathbb{M}\mathbf{R}$ in Eq.6 are Hermitian therefore their resulting eigenvectors will be orthogonal. Eigenvalue sensitivity for both undamped and damped systems is an established result in modern literature [13, 15] that will be employed in the present work. When the partial derivatives

4

of $\mathbf{K}$, $\mathbf{C}$, $\mathbf{M}$ with regard to design parameters β_i, β_j are known then the sensitivity of an eigenvalue λ_w to this design parameter for a damped system will be equal to

$$\frac{\partial \lambda_w}{\partial \beta_i} = -\frac{\mathbf{x}_w^\top \left(\lambda_w^2 \frac{\partial \mathbf{M}}{\partial \beta_i} + \lambda_w \frac{\partial \mathbf{C}}{\partial \beta_i} + \frac{\partial \mathbf{K}}{\partial \beta_i} \right) \mathbf{x}_w}{\mathbf{x}_w^\top \left(2\lambda_w \mathbf{M} + \mathbf{C} \right) \mathbf{x}_w} \tag{7a}$$

$$\frac{\partial^2 \lambda_w}{\partial \beta_j \partial \beta_i} = -\frac{1}{\mathbf{x}_w^\top \left(2\lambda_w \mathbf{M} + \mathbf{C} \right) \mathbf{x}_w} \times \tag{7b}$$

$$\times \left[\mathbf{x}_w^\top \left(\lambda_w^2 \frac{\partial^2 \mathbf{M}}{\partial \beta_j \partial \beta_i} + \lambda_w \frac{\partial^2 \mathbf{C}}{\partial \beta_j \partial \beta_i} + \frac{\partial^2 \mathbf{K}}{\partial \beta_j \partial \beta_i} + \frac{\partial \lambda_w}{\partial \beta_i} \left(2\lambda_w \frac{\partial \mathbf{M}}{\partial \beta_j} + \frac{\partial \mathbf{C}}{\partial \beta_j} \right) + \frac{\partial \lambda_w}{\partial \beta_j} \left(2\lambda_w \frac{\partial \mathbf{M}}{\partial \beta_i} + \frac{\partial \mathbf{C}}{\partial \beta_i} \right) \right) \mathbf{x}_w \right.$$

$$+ \mathbf{x}_w^\top \left(\lambda_w^2 \frac{\partial \mathbf{M}}{\partial \beta_i} + \lambda_w \frac{\partial \mathbf{C}}{\partial \beta_i} + \frac{\partial \mathbf{K}}{\partial \beta_i} + \frac{\partial \lambda_w}{\partial \beta_i} \left(2\lambda_w \mathbf{M} + \mathbf{C} \right) \right) \frac{\partial \mathbf{x}_w}{\partial \beta_j}$$

$$\left. + \mathbf{x}_w^\top \left(\lambda_w^2 \frac{\partial \mathbf{M}}{\partial \beta_j} + \lambda_w \frac{\partial \mathbf{C}}{\partial \beta_j} + \frac{\partial \mathbf{K}}{\partial \beta_j} + \frac{\partial \lambda_w}{\partial \beta_j} \left(2\lambda_w \mathbf{M} + \mathbf{C} \right) \right) \frac{\partial \mathbf{x}_w}{\partial \beta_i} + 2 \frac{\partial \lambda_w}{\partial \beta_i} \frac{\partial \lambda_w}{\partial \beta_j} \mathbf{x}_w^\top \mathbf{M} \mathbf{x}_w \right]$$

with the first order sensitivity of the resulting eigenvectors being computed as

$$\frac{\partial \mathbf{x}_w}{\partial \beta_i} = -\frac{1}{4\lambda_w} \left(\mathbf{x}_w^\top \left(2\lambda_w \frac{\partial \mathbf{M}}{\partial \beta_j} + \frac{\partial \mathbf{C}}{\partial \beta_j} \right) \mathbf{x}_w \right) \mathbf{x}_w \tag{8a}$$

$$- \frac{1}{2\lambda_w^*} \frac{\left(\mathbf{x}_w^* - \left(\frac{1}{2\lambda_w} \mathbf{x}_w^{*\top} \left((\lambda_w + \lambda_w^*) \mathbf{M} + \mathbf{C} \right) \mathbf{x}_w \right) \mathbf{x}_w \right)^\top \left(\lambda_w^2 \frac{\partial \mathbf{M}}{\partial \beta_i} + \lambda_w \frac{\partial \mathbf{C}}{\partial \beta_i} + \frac{\partial \mathbf{K}}{\partial \beta_i} \right) \mathbf{x}_w}{2 \mathscr{I}(\lambda_w)} \mathbf{x}_w^*$$

$$- \sum_{\substack{m=1 \\ m \neq w}}^{m_{max}} \left[\frac{1}{2\lambda_m} \frac{\mathbf{x}_{0m}^\top \left(\lambda_w^2 \frac{\partial \mathbf{M}}{\partial \beta_i} + \lambda_w \frac{\partial \mathbf{C}}{\partial \beta_i} + \frac{\partial \mathbf{K}}{\partial \beta_i} \right) \mathbf{x}_w}{\lambda_w - \lambda_m} \mathbf{x}_m + \frac{1}{2\lambda_m^*} \frac{\mathbf{x}_m^{*\top} \left(\lambda_w^2 \frac{\partial \mathbf{M}}{\partial \beta_i} + \lambda_w \frac{\partial \mathbf{C}}{\partial \beta_i} + \frac{\partial \mathbf{K}}{\partial \beta_i} \right) \mathbf{x}_w}{\lambda_w - \lambda_m^*} \mathbf{x}_m^* \right]$$

with $\mathscr{I}(\cdot)$ denoting the imaginary part, λ_w a known eigenvalue of the system having the corresponding complex eigenvector $\mathbf{x}_w$.

2.2.2. Conservative structural system

For an undamped structural segment having $\mathbf{C} = \mathbf{0}$ the above expressions, this time concerning the sensitivity of the real eigenvalues λ_w become

$$\frac{\partial \lambda_w}{\partial \beta_i} = \mathbf{x}_w^\top \left(\frac{\partial \mathbf{K}}{\partial \beta_i} - \lambda_w \frac{\partial \mathbf{M}}{\partial \beta_i} \right) \mathbf{x}_w \tag{9a}$$

$$\frac{\partial^2 \lambda_w}{\partial \beta_j \partial \beta_i} = \mathbf{x}_w^\top \left(\frac{\partial^2 \mathbf{K}}{\partial \beta_j \partial \beta_i} - \lambda_w \frac{\partial^2 \mathbf{M}}{\partial \beta_j \partial \beta_i} - \frac{\partial \lambda_w}{\partial \beta_j} \frac{\partial \mathbf{M}}{\partial \beta_i} - \frac{\partial \lambda_w}{\partial \beta_i} \frac{\partial \mathbf{M}}{\partial \beta_j} \right) \mathbf{x}_w \tag{9b}$$

$$+ \mathbf{x}_w^\top \left(\frac{\partial}{\partial \beta_j} \left[\mathbf{K} - \lambda_w \mathbf{M} \right] \right) \frac{\partial \mathbf{x}_w}{\partial \beta_i} + \mathbf{x}_w^\top \left(\frac{\partial}{\partial \beta_i} \left[\mathbf{K} - \lambda_w \mathbf{M} \right] \right) \frac{\partial \mathbf{x}_w}{\partial \beta_j}$$

with the sensitivity of the real mode shapes $\frac{\partial \mathbf{x}_w}{\partial \beta_j}$ to be calculated by the approach exhibited in [13]. The global mass and stiffness matrices $\mathbb{M}$, $\mathbb{K}$ of the structural segment are formed by adding the local mass and stiffness matrices of

individual FEs. It is therefore evident that when the expression of the partial derivatives for every local mass, damping and stiffness matrix $\dfrac{\partial \mathbf{m}}{\partial \beta_i}, \dfrac{\partial \mathbf{c}}{\partial \beta_i}, \dfrac{\partial \mathbf{k}}{\partial \beta_i}$ and $\dfrac{\partial^2 \mathbf{m}}{\partial \beta_j \partial \beta_i}, \dfrac{\partial^2 \mathbf{c}}{\partial \beta_j \partial \beta_i}, \dfrac{\partial^2 \mathbf{k}}{\partial \beta_j \partial \beta_i}$ are known then the expressions for the global matrices $\dfrac{\partial \mathbb{M}}{\partial \beta_i}, \dfrac{\partial \mathbb{C}}{\partial \beta_i}, \dfrac{\partial \mathbb{K}}{\partial \beta_i}$ and $\dfrac{\partial^2 \mathbb{M}}{\partial \beta_j \partial \beta_i}, \dfrac{\partial^2 \mathbb{C}}{\partial \beta_j \partial \beta_i}, \dfrac{\partial^2 \mathbb{K}}{\partial \beta_j \partial \beta_i}$ can be derived simply by adding the expressions of the local matrices together. Eq.9 can therefore be written as

$$\frac{\partial \lambda_w}{\partial \beta_i} = \mathbf{x}_w^\top \left(\mathbf{R}^* \frac{\partial \mathbb{K}}{\partial \beta_i} \mathbf{R} - \lambda_w \mathbf{R}^* \frac{\partial \mathbb{M}}{\partial \beta_i} \mathbf{R} \right) \mathbf{x}_w \tag{10a}$$

$$\frac{\partial^2 \lambda_w}{\partial \beta_j \partial \beta_i} = \mathbf{x}_w^\top \left(\mathbf{R}^* \frac{\partial^2 \mathbb{K}}{\partial \beta_j \partial \beta_i} \mathbf{R} - \lambda_w \mathbf{R}^* \frac{\partial^2 \mathbb{M}}{\partial \beta_j \partial \beta_i} \mathbf{R} - \mathbf{R}^* \frac{\partial \lambda_w}{\partial \beta_j} \frac{\partial \mathbb{M}}{\partial \beta_i} \mathbf{R} - \mathbf{R}^* \frac{\partial \lambda_w}{\partial \beta_i} \frac{\partial \mathbb{M}}{\partial \beta_j} \mathbf{R} \right) \mathbf{x}_w + \tag{10b}$$

$$\mathbf{x}_w^\top \left(\frac{\partial}{\partial \beta_j} \left[\mathbf{R}^* \mathbb{K} \mathbf{R} - \lambda_w \mathbf{R}^* \mathbb{M} \mathbf{R} \right] \right) \frac{\partial \mathbf{x}_w}{\partial \beta_i} + \mathbf{x}_w^\top \left(\frac{\partial}{\partial \beta_i} \left[\mathbf{R}^* \mathbb{K} \mathbf{R} - \lambda_w \mathbf{R}^* \mathbb{M} \mathbf{R} \right] \right) \frac{\partial \mathbf{x}_w}{\partial \beta_j}$$

For the conservative system it is known however that $\dfrac{\partial \lambda_w}{\partial \beta_i} = \dfrac{\partial (\omega_w^2)}{\partial \beta_i}$, therefore

$$\frac{\partial \lambda_w}{\partial \beta_i} = \frac{\dfrac{\partial (\omega_w^2)}{\partial \omega_w}}{\dfrac{\partial \beta_i}{\partial \omega_w}} = 2\omega_w \frac{\partial \omega_w}{\partial \beta_i} \Leftrightarrow \frac{\partial \omega_w}{\partial \beta_i} = \frac{1}{2\omega_w} \frac{\partial \lambda_w}{\partial \beta_i} \tag{11a}$$

$$\frac{\partial^2 \lambda_w}{\partial \beta_j \partial \beta_i} = 2 \frac{\partial \omega_w}{\partial \beta_j} \frac{\partial \omega_w}{\partial \beta_i} + 2\omega_w \frac{\partial^2 \omega_w}{\partial \beta_j \partial \beta_i} \Leftrightarrow \frac{\partial^2 \omega_w}{\partial \beta_j \partial \beta_i} = \frac{1}{2\omega_w} \left(\frac{\partial^2 \lambda_w}{\partial \beta_j \partial \beta_i} - 2 \frac{\partial \omega_w}{\partial \beta_j} \frac{\partial \omega_w}{\partial \beta_i} \right) \tag{11b}$$

with ω_w the angular frequency at which the set of ε_x, ε_y is true for the w wave type described by the $\mathbf{x}_w$ deformation. For the wavenumber sensitivity $\dfrac{\partial k_w}{\partial \beta_i}$ the following is true

$$\frac{\partial k_w}{\partial \beta_i} = -\frac{\partial k_w}{\partial \omega_w} \frac{\partial \omega_w}{\partial \beta_i} = -\frac{1}{c_{g,w}} \frac{\partial \omega_w}{\partial \beta_i} \tag{12a}$$

$$\frac{\partial^2 k_w}{\partial \beta_j \partial \beta_i} = \frac{1}{c_{g,w}^3} \frac{\partial c_{g,w}}{\partial k_w} \frac{\partial \omega_w}{\partial \beta_j} \frac{\partial \omega_w}{\partial \beta_i} - \frac{1}{c_{g,w}} \frac{\partial^2 \omega_w}{\partial \beta_j \partial \beta_i} \tag{12b}$$

with $c_{g,w} = \dfrac{\partial \omega_w}{\partial k_w}$ the group velocity associated with the wave type w at frequency ω_w and the quantities $c_{g,w}$, $\dfrac{\partial c_{g,w}}{\partial \omega_w}$ to be numerically evaluated by the solution of the baseline structural design. The generic symbolic expressions of the $\mathbf{m}, \mathbf{c}, \mathbf{k}$ matrices for an orthotropic structural segment modelled with a linear solid FE is given in Appendix A.

3. SEA sensitivity analysis

3.1. The employed SEA model

The impact of the parametric alterations on the vibroacoustic performance of the structure under investigation is exhibited in this section by deriving expressions for the sensitivity of the SEA results with respect to the propagating acoustic waves.

The total acoustic transmission coefficient τ is one of the most important indices of the vibroacoustic performance of a structure. The system to be modelled comprises one acoustically excited chamber (subsystem 1) and one acoustically receiving chamber (subsystem 3) separated by the modelled composite panel (subsystem 2). It is considered that each wave type is excited and transmits acoustic energy independently from the rest, therefore each considered wave type $w = w_1, w_2...w_n$ propagating within the composite panel is considered as a separate SEA subsystem. No flanking transmission is considered in the SEA model. The energy balance between the subsystems as it is considered within an SEA approach (see [7]) is illustrated in Fig.2, in which E_1, E_3 stand for the acoustic energy of the source room and the receiving room respectively and E_2 for the vibrational energy of the composite panel. Moreover P_{in} is the injected power in the source room, P_{1d}, P_{2d} and P_{3d} stand for the power dissipated by each subsystem and P_{13} is the non-resonant transmitted power between the rooms.

[Figure 2 about here.]

The derivation of an expression for the total acoustic transmission coefficient τ of the composite structure by merely accounting for its structural dynamic behaviour is summarized in Appendix B (as exhibited in [11]) and reads

$$\tau = \sum_{w=w_1}^{w_n} \tau_w + \frac{P_{13}}{P_{inc}} \tag{13}$$

with τ_w being the transmission coefficient of the wave type w given as

$$\tau_w = \frac{8\rho^2 c^4 \pi \sigma_{rad,w}^2 n_w}{\rho_s \omega^2 A(\rho_s \omega \eta_w + 2\rho c \sigma_{rad,w})} \tag{14}$$

The non resonant transmission coefficient $\tau_{nr} = P_{13}/P_{inc}$ for a diffused acoustic field can be written as in [9]:

$$\tau_{nr}(\omega) = \frac{1}{\pi(\cos^2 \theta_{min} - \cos^2 \theta_{max})} \int_0^{2\pi} \int_0^{\theta_{max}} \frac{4Z_0^2}{\mid i\omega\rho_s + 2Z_0 \mid^2} \sigma(\theta, \phi, \omega) \cos^2 \theta \sin \theta d\theta d\phi \tag{15}$$

in which θ and ϕ are the incidence angle and the direction angle of the acoustic wave respectively and $Z_0 = \rho c/\cos\theta$ is the acoustic impedance of the medium. The term θ_{max} stands for the maximum incidence angle, accounting for the diffuseness of the incident field. It is hereby considered that $\theta_{max} = \pi/2$ for all the results presented in the current work. The term $\sigma(\theta, \phi, \omega)$ is the corrected radiation efficiency term. It is used in order to account for the finite dimensions of the panel and it is calculated using a spatial windowing correction technique presented in [30].

Eventually the STL of the panel can be expressed as

$$STL = 10 \log_{10}\left(\frac{1}{\tau}\right) \tag{16}$$

by definition.

3.2. Parametric sensitivity of the total acoustic transmission

In order to formulate the expression of the Hessian matrix describing the variation of the vibroacoustic performance of the structure with respect to its design parameters, the second order derivative of τ with respect to the considered set of parameters should be derived and expressed as

$$\frac{\partial \tau}{\partial \beta_i} = \sum_{w=w_1}^{w_n} \frac{\partial \tau_w}{\partial \beta_i} + \frac{\partial \tau_{nr}}{\partial \beta_i} \tag{17a}$$

$$\frac{\partial^2 \tau}{\partial \beta_j \partial \beta_i} = \sum_{w=w_1}^{w_n} \frac{\partial^2 \tau_w}{\partial \beta_j \partial \beta_i} + \frac{\partial^2 \tau_{nr}}{\partial \beta_j \partial \beta_i} \tag{17b}$$

while the sensitivity of the STL index can directly be expressed with regard to τ as

$$\frac{\partial (STL)}{\partial \beta_i} = \frac{\mathrm{d}(STL)}{\mathrm{d}\tau} \frac{\partial \tau}{\partial \beta_i} = -\frac{10}{\ln(10)\tau} \frac{\partial \tau}{\partial \beta_i} \tag{18a}$$

$$\frac{\partial^2 (STL)}{\partial \beta_j \partial \beta_i} = \frac{\partial^2 (STL)}{\partial \tau^2} \frac{\partial \tau}{\partial \beta_j} \frac{\partial \tau}{\partial \beta_i} + \frac{\partial (STL)}{\partial \tau} \frac{\partial^2 \tau}{\partial \beta_j \partial \beta_i} \tag{18b}$$

$$= \frac{10}{\ln(10)\tau^2} \frac{\partial \tau}{\partial \beta_j} \frac{\partial \tau}{\partial \beta_i} - \frac{10}{\ln(10)\tau} \frac{\partial^2 \tau}{\partial \beta_j \partial \beta_i}$$

In the following sections the evaluation of Eq.17 is discussed.

3.3. Modal density sensitivity

Using Courant's formula [31], the modal density of each wave type w can be written at a propagation angle ϕ as a function of the propagating wavenumber and its corresponding group velocity c_g:

$$n_w(\omega, \phi) = \frac{A k_w(\omega, \phi)}{2\pi^2 |c_{g,w}(\omega, \phi)|} \tag{19}$$

The angularly averaged modal density of the structure is therefore given as

$$n_w(\omega) = \int_0^\pi n_w(\omega, \phi) \, \mathrm{d}\phi \tag{20}$$

Thanks to the chain differentiation rule the first and second order derivatives of the modal density for each wave type with respect to design variables β_i, β_j can be expressed as

8

$$\frac{\partial n_w(\omega,\phi)}{\partial \beta_i} = \frac{\partial n_w(\omega,\phi)}{\partial k_w(\omega,\phi)}\frac{\partial k_w(\omega,\phi)}{\partial \beta_i} + \frac{\partial n_w(\omega,\phi)}{\partial c_{g,w}(\omega,\phi)}\frac{\partial c_{g,w}(\omega,\phi)}{\partial \beta_i} \tag{21a}$$

$$= \frac{A}{2\pi^2|c_{g,w}(\omega,\phi)|}\frac{\partial k_w(\omega,\phi)}{\partial \beta_i} - \frac{Ak_w(\omega,\phi)\,\mathrm{sgn}(c_{g,w}(\omega,\phi))}{2\pi^2|c_{g,w}(\omega,\phi)|^2}\frac{\partial c_{g,w}(\omega,\phi)}{\partial k_w(\omega,\phi)}\frac{\partial k_w(\omega,\phi)}{\partial \beta_i}$$

$$\frac{\partial^2 n_w(\omega,\phi)}{\partial \beta_j \partial \beta_i} = \frac{\partial^2 n_w(\omega,\phi)}{\partial k_w(\omega,\phi)^2}\frac{\partial k_w(\omega,\phi)}{\partial \beta_j}\frac{\partial k_w(\omega,\phi)}{\partial \beta_i} + \frac{\partial n_w(\omega,\phi)}{\partial k_w(\omega,\phi)}\frac{\partial^2 k_w(\omega,\phi)}{\partial \beta_j \partial \beta_i} \tag{21b}$$

$$+ \frac{\partial^2 n_w(\omega,\phi)}{\partial c_{g,w}(\omega,\phi)^2}\frac{\partial c_{g,w}(\omega,\phi)}{\partial \beta_j}\frac{\partial c_{g,w}(\omega,\phi)}{\partial \beta_i} + \frac{\partial n_w(\omega,\phi)}{\partial c_{g,w}(\omega,\phi)}\frac{\partial^2 c_{g,w}(\omega,\phi)}{\partial \beta_j \partial \beta_i}$$

$$= \frac{A}{2\pi^2|c_{g,w}(\omega,\phi)|}\frac{\partial^2 k_w(\omega,\phi)}{\partial \beta_j \partial \beta_i} + \frac{Ak_w(\omega,\phi)\,\mathrm{sgn}(c_{g,w}(\omega,\phi))}{\pi^2|c_{g,w}(\omega,\phi)|^3}\left(\frac{\partial c_{g,w}(\omega,\phi)}{\partial k_w(\omega,\phi)}\right)^2\frac{\partial k_w(\omega,\phi)}{\partial \beta_j}\frac{\partial k_w(\omega,\phi)}{\partial \beta_i}$$

$$- \frac{Ak_w(\omega,\phi)\,\mathrm{sgn}(c_{g,w}(\omega,\phi))}{2\pi^2|c_{g,w}(\omega,\phi)|^2}\left(\frac{\partial^2 c_{g,w}(\omega,\phi)}{\partial k_w(\omega,\phi)^2}\frac{\partial k_w(\omega,\phi)}{\partial \beta_j}\frac{\partial k_w(\omega,\phi)}{\partial \beta_i} + \frac{\partial c_{g,w}(\omega,\phi)}{\partial k_w(\omega,\phi)}\frac{\partial^2 k_w(\omega,\phi)}{\partial \beta_j \partial \beta_i}\right)$$

while for the spatially averaged modal density

$$\frac{\partial n_w(\omega)}{\partial \beta_i} = \int_0^\pi \frac{\partial n_w(\omega,\phi)}{\partial \beta_i}\mathrm{d}\phi \tag{22a}$$

$$\frac{\partial^2 n_w(\omega)}{\partial \beta_j \partial \beta_i} = \int_0^\pi \frac{\partial^2 n_w(\omega,\phi)}{\partial \beta_j \partial \beta_i}\mathrm{d}\phi \tag{22b}$$

suggesting that the modal density sensitivity can be expressed merely by

- The sensitivity of the characteristics of the waves travelling within the considered structure with respect to the structural design (already determined in Sec.2).

- The sensitivity of the modal density with respect to the characteristics of the waves travelling in it.

A similar approach will be followed for computing all the remaining necessary quantities throughout this work. It should be noted that Eq.21 is derived under the assumption that $c_{g,w}(\omega,\phi) \neq 0$

3.4. Radiation efficiency sensitivity

In order to avoid the computationally inefficient frequency and directional averaging of the modal dependent radiation efficiency sensitivity $\frac{\partial \sigma_{rad,w}(\omega,\phi)}{\partial \beta_i}$, it is practical to employ expressions introducing a direct wavenumber dependence of $\sigma_{rad,w}$ such as the ones exhibited in [5, 8, 10]. For a generic periodic structure including discontinuities the assumption of sinusoidal mode shapes is no longer valid, therefore the radiation efficiency should be calculated directly from the PST derived wave mode shapes. The radiation efficiency expression as derived in [10] can therefore be employed. For continuous structures, mode shapes of sinusoidal form can be assumed in order to avoid any FE discretization errors in the solution. The set of asymptotic formulas given in [8] can be used for computing the averaged wavenumber dependent radiation efficiency of the panel as

$$\sigma_{rad,w}(k(\omega)) = \begin{cases} \dfrac{1}{\sqrt{1-\mu^2}} & \mu < 1 \\[2ex] \dfrac{L_x + L_y}{\pi\mu\kappa L_x L_y \sqrt{\mu^2 - 1}} \left(\ln\left(\dfrac{\mu+1}{\mu-1}\right) + \dfrac{2\mu}{\mu^2-1}\right) & \mu > 1 \end{cases}$$

with $\mu = \left(\dfrac{k_x^2 + k_y^2}{\kappa^2}\right)^{1/2}$, where $\kappa = \omega/c$ is the acoustic wavenumber. It is noted that the above expressions are largely overestimating the radiation efficiency of the structure close to the coincidence frequency. An efficient approximation of $\sigma_{rad,w}$ when $k = \kappa$ is given in [8] as

$$\sigma_{rad,w}(k(\omega)) = \left(0.5 - 0.15\min(L_x, L_y)/\max(L_x, L_y)\right)\sqrt{k\min(L_x, L_y)}$$

Three domains will therefore be distinguished for the radiation efficiency of the panel. It has been empirically observed that the above cited relations overestimate the radiation efficiency of the panel within a region $0.90 < \mu < 1.05$. The following relations for $\sigma_{rad,w}(k(\omega))$ are therefore hereby suggested

$$\sigma_{rad,w} = \frac{1}{\sqrt{1-\mu^2}} \quad \mu < 0.90 \tag{23a}$$

$$\sigma_{rad,w} = \frac{L_x + L_y}{\pi\mu\kappa L_x L_y \sqrt{\mu^2 - 1}}\left(\ln\left(\frac{\mu+1}{\mu-1}\right) + \frac{2\mu}{\mu^2-1}\right) \quad \mu > 1.05 \tag{23b}$$

$$\sigma_{rad,w} = \left(0.5 - 0.15\min(L_x, L_y)/\max(L_x, L_y)\right)\sqrt{k\min(L_x, L_y)} \quad \mu = 1 \tag{23c}$$

In the region $0.90 < \mu < 1.05$ a shape preserving Hermite interpolation function is employed assuring the continuity and double differentiability for the entire spectrum of the $\sigma_{rad,w}$ expression. The sensitivity expressions can therefore be directly derived by Eq.23 in the $\mu < 0.90$ and $\mu > 1.05$ regions as

$$\frac{\partial \sigma_{rad,w}}{\partial \beta_i} = \frac{\partial \sigma_{rad,w}}{\partial k_w} \frac{\partial k_w}{\partial \beta_i} = \frac{k_w}{\kappa^2(1 - k_w^2/\kappa^2)^{3/2}} \frac{\partial k_w}{\partial \beta_i} \quad \mu < 0.90 \tag{24a}$$

$$\frac{\partial^2 \sigma_{rad,w}}{\partial \beta_j \partial \beta_i} = \frac{\partial^2 \sigma_{rad,w}}{\partial k_w^2} \frac{\partial k_w}{\partial \beta_j} \frac{\partial k_w}{\partial \beta_i} + \frac{\partial \sigma_{rad,w}}{\partial k_w} \frac{\partial^2 k_w}{\partial \beta_j \partial \beta_i} \tag{24b}$$

$$= \left(\frac{1}{\kappa^2(1 - k_w^2/\kappa^2)^{3/2}} + \frac{3k_w^2}{\kappa^4(1 - k_w^2/\kappa^2)^{5/2}} \right) \frac{\partial k_w}{\partial \beta_j} \frac{\partial k_w}{\partial \beta_i} + \frac{k_w}{\kappa^2(1 - k_w^2/\kappa^2)^{3/2}} \frac{\partial^2 k_w}{\partial \beta_j \partial \beta_i} \quad \mu < 0.90$$

$$\frac{\partial \sigma_{rad,w}}{\partial \beta_i} = -\frac{4k_w(L_x + L_y)}{\pi L_x L_y \kappa^3((k_w^2 - \kappa^2)/\kappa^2)^{5/2}} \frac{\partial k_w}{\partial \beta_i} \tag{24c}$$

$$- \frac{k_w(L_x + L_y) \left(\ln \frac{\mu + 1}{\mu - 1} + (2\kappa^2\mu)/(k_w^2 - \kappa^2) \right)}{\pi L_x L_y \kappa^3((k_w^2 - \kappa^2)/\kappa^2)^{1/2}(k_w^2/\kappa^2)^{3/2}} \frac{\partial k_w}{\partial \beta_i}$$

$$- \frac{k_w(L_x + L_y) \left(\ln \frac{\mu + 1}{\mu - 1} + (2\kappa^2\mu)/(k_w^2 - \kappa^2) \right)}{\pi L_x L_y \kappa^3((k_w^2 - \kappa^2)/\kappa^2)^{3/2}\mu} \frac{\partial k_w}{\partial \beta_i} \quad \mu > 1.05$$

$$\frac{\partial^2 \sigma_{rad,w}}{\partial \beta_j \partial \beta_i} = \frac{k_w^2(L_x + L_y)(4\kappa^6\mu + 6k_w^6 \ln \frac{\mu + 1}{\mu - 1} - 2\kappa^6 \ln \frac{\mu + 1}{\mu - 1} - 10k_w^2\kappa^4\mu)}{\pi L_x L_y \kappa^{11}((k_w^2 - \kappa^2)/\kappa^2)^{7/2}(k_w^2/\kappa^2)^{5/2}} \frac{\partial k_w}{\partial \beta_j} \frac{\partial k_w}{\partial \beta_i} \tag{24d}$$

$$+ \frac{k_w^2(L_x + L_y)(36k_w^4\kappa^2\mu + 7k_w^2\kappa^4 \ln \frac{\mu + 1}{\mu - 1} - 11k_w^4\kappa^2 \ln \frac{\mu + 1}{\mu - 1})}{\pi L_x L_y \kappa^{11}((k_w^2 - \kappa^2)/\kappa^2)^{7/2}(k_w^2/\kappa^2)^{5/2}} \frac{\partial k_w}{\partial \beta_j} \frac{\partial k_w}{\partial \beta_i}$$

$$- \frac{4k_w(L_x + L_y)}{\pi L_x L_y \kappa^3((k_w^2 - \kappa^2)/\kappa^2)^{5/2}} \frac{\partial^2 k_w}{\partial \beta_j \partial \beta_i}$$

$$- \frac{k_w(L_x + L_y) \left(\ln \frac{\mu + 1}{\mu - 1} + (2\kappa^2\mu)/(k_w^2 - \kappa^2) \right)}{\pi L_x L_y \kappa^3((k_w^2 - \kappa^2)/\kappa^2)^{1/2}(k_w^2/\kappa^2)^{3/2}} \frac{\partial^2 k_w}{\partial \beta_j \partial \beta_i}$$

$$- \frac{k_w(L_x + L_y) \left(\ln \frac{\mu + 1}{\mu - 1} + (2\kappa^2\mu)/(k_w^2 - \kappa^2) \right)}{\pi L_x L_y \kappa^3((k_w^2 - \kappa^2)/\kappa^2)^{3/2}\mu} \frac{\partial^2 k_w}{\partial \beta_j \partial \beta_i} \quad \mu > 1.05$$

while the interpolation function is used for expressing the sensitivity of $\sigma_{rad,w}$ for the remaining spectrum.

3.5. Damping loss factor sensitivity

Reducing the acoustic transparency of a structural panel by increasing its intrinsic damping properties is a popular noise reduction strategy within the modern industry and oftentimes an effective option, particularly in the high frequency range. It is therefore particularly useful to develop dedicated models for evaluating the effect of the increase of the damping coefficient γ of the material comprised in a single layer of the composite structure on its total loss factor. Having a look at the form of the eigenvalue problem in Eq.6 it can be deduced that expressing the total loss factor of the structural panel as a function of the real and imaginary parts of the resulting eigenvalues (as in [32, 33]) can be particularly practical.

The loss factor of each computed wave type w can directly be determined as

$$\eta_w(\omega, \phi) = 2\frac{\omega_i \omega_r}{\omega_r^2 - \omega_i^2} \tag{25}$$

with $\eta_n(\omega, \phi)$ the loss factor for the wave type w at a certain angular frequency ω and propagating towards a certain direction ϕ. The total frequency dependent loss factor of a certain wavetype can be computed as

$$\eta_w(\omega) = \frac{\int_0^\pi \eta_n(\omega, \phi) \mathrm{d}\phi}{\pi} \tag{26}$$

which can be evaluated at the entire spectrum of interest. The sensitivity of the directional loss factor $\eta_w(\omega, \phi)$ can therefore be expressed as

$$\frac{\partial \eta_w(\omega, \phi)}{\partial \beta_i} = \frac{\partial \eta_w(\omega, \phi)}{\partial \omega_r(\omega, \phi)} \frac{\partial \omega_r(\omega, \phi)}{\partial \beta_i} + \frac{\partial \eta_w(\omega, \phi)}{\partial \omega_i(\omega, \phi)} \frac{\partial \omega_i(\omega, \phi)}{\partial \beta_i} \tag{27a}$$

$$= -\left(\frac{2\omega_i}{\omega_i^2 - \omega_r^2} + \frac{4\omega_i \omega_r^2}{(\omega_i^2 - \omega_r^2)^2}\right)\frac{\partial \omega_r(\omega, \phi)}{\partial \beta_i} + \left(\frac{4\omega_i^2 \omega_r}{(\omega_i^2 - \omega_r^2)^2} - \frac{2\omega_r}{\omega_i^2 - \omega_r^2}\right)\frac{\partial \omega_i(\omega, \phi)}{\partial \beta_i}$$

$$\frac{\partial^2 \eta_w(\omega, \phi)}{\partial \beta_j \partial \beta_i} = \frac{\partial^2 \eta_w(\omega, \phi)}{\partial \omega_r(\omega, \phi)^2}\frac{\partial \omega_r(\omega, \phi)}{\partial \beta_j}\frac{\partial \omega_r(\omega, \phi)}{\partial \beta_i} + \frac{\partial \eta_w(\omega, \phi)}{\partial \omega_r(\omega, \phi)}\frac{\partial^2 \omega_r(\omega, \phi)}{\partial \beta_j \partial \beta_i} \tag{27b}$$

$$+ \frac{\partial^2 \eta_w(\omega, \phi)}{\partial \omega_i(\omega, \phi)^2}\frac{\partial \omega_i(\omega, \phi)}{\partial \beta_j}\frac{\partial \omega_i(\omega, \phi)}{\partial \beta_i} + \frac{\partial \eta_w(\omega, \phi)}{\partial \omega_i(\omega, \phi)}\frac{\partial^2 \omega_i(\omega, \phi)}{\partial \beta_j \partial \beta_i}$$

$$= -\left(\frac{16\omega_i \omega_r^3}{(\omega_i^2 - \omega_r^2)^3} + \frac{12\omega_i \omega_r}{(\omega_i^2 - \omega_r^2)^2}\right)\frac{\partial \omega_r(\omega, \phi)}{\partial \beta_j}\frac{\partial \omega_r(\omega, \phi)}{\partial \beta_i} - \left(\frac{2\omega_i}{\omega_i^2 - \omega_r^2} + \frac{4\omega_i \omega_r^2}{(\omega_i^2 - \omega_r^2)^2}\right)\frac{\partial^2 \omega_r(\omega, \phi)}{\partial \beta_j \partial \beta_i}$$

$$+ \left(\frac{12\omega_i \omega_r}{(\omega_i^2 - \omega_r^2)^2} - \frac{16\omega_i^3 \omega_r}{(\omega_i^2 - \omega_r^2)^3}\right)\frac{\partial \omega_i(\omega, \phi)}{\partial \beta_j}\frac{\partial \omega_i(\omega, \phi)}{\partial \beta_i} + \left(\frac{4\omega_i^2 \omega_r}{(\omega_i^2 - \omega_r^2)^2} - \frac{2\omega_r}{\omega_i^2 - \omega_r^2}\right)\frac{\partial^2 \omega_i(\omega, \phi)}{\partial \beta_j \partial \beta_i}$$

while for the total loss factor of the panel

$$\frac{\partial \eta_w(\omega)}{\partial \beta_i} = \int_0^\pi \frac{1}{\pi}\frac{\partial \eta_w(\omega, \phi)}{\partial \beta_i}\mathrm{d}\phi \tag{28a}$$

$$\frac{\partial^2 \eta_w(\omega)}{\partial \beta_j \partial \beta_i} = \int_0^\pi \frac{1}{\pi}\frac{\partial^2 \eta_w(\omega, \phi)}{\partial \beta_j \partial \beta_i}\mathrm{d}\phi \tag{28b}$$

to be evaluated in the frequency bands of interest.

3.6. Sensitivity of the resonant acoustic transmission

Taking a look at Eq.14 it can be observed that the sensitivity of the resonant acoustic transmission coefficient with respect to the design parameters of the composite structure can be expressed as

$$\frac{\partial \tau_w}{\partial \beta_i} = \frac{\partial \tau_w}{\partial \sigma_{rad,w}}\frac{\partial \sigma_{rad,w}}{\partial \beta_i} + \frac{\partial \tau_w}{\partial n_w}\frac{\partial n_w}{\partial \beta_i} + \frac{\partial \tau_w}{\partial \eta_w}\frac{\partial \eta_w}{\partial \beta_i} + \frac{\partial \tau_w}{\partial \rho_s}\frac{\partial \rho_s}{\partial \beta_i} \tag{29a}$$

$$\frac{\partial^2 \tau_w}{\partial \beta_j \partial \beta_i} = \frac{\partial^2 \tau_w}{\partial \sigma_{rad,w}^2}\frac{\partial \sigma_{rad,w}}{\partial \beta_j}\frac{\partial \sigma_{rad,w}}{\partial \beta_i} + \frac{\partial \tau_w}{\partial \sigma_{rad,w}}\frac{\partial^2 \sigma_{rad,w}}{\partial \beta_j \partial \beta_i} \tag{29b}$$

$$+ \frac{\partial^2 \tau_w}{\partial n_w^2}\frac{\partial n_w}{\partial \beta_j}\frac{\partial n_w}{\partial \beta_i} + \frac{\partial \tau_w}{\partial n_w}\frac{\partial^2 n_w}{\partial \beta_j \partial \beta_i}$$

$$+ \frac{\partial^2 \tau_w}{\partial \eta_w^2}\frac{\partial \eta_w}{\partial \beta_j}\frac{\partial \eta_w}{\partial \beta_i} + \frac{\partial \tau_w}{\partial \eta_w}\frac{\partial^2 \eta_w}{\partial \beta_j \partial \beta_i}$$

$$+ \frac{\partial^2 \tau_w}{\partial \rho_s^2}\frac{\partial \rho_s}{\partial \beta_j}\frac{\partial \rho_s}{\partial \beta_i} + \frac{\partial \tau_w}{\partial \rho_s}\frac{\partial^2 \rho_s}{\partial \beta_j \partial \beta_i}$$

with the transmission coefficient related sensitivity terms being expressed as

$$\frac{\partial \tau_w}{\partial \sigma_{rad,w}} = \frac{16\pi c^4 n_w \rho^2 \sigma_{rad,w}}{A\omega^2 \rho_s (\eta_w \omega \rho_s + 2c\rho\sigma_{rad,w})} - \frac{16\pi c^5 n_w \rho^3 \sigma_{rad,w}^2}{A\omega^2 \rho_s (\eta_w \omega \rho_s + 2c\rho\sigma_{rad,w})^2} \tag{30a}$$

$$\frac{\partial^2 \tau_w}{\partial \sigma_{rad,w}^2} = \frac{16\pi c^4 n_w \rho^2}{A\omega^2 \rho_s (\eta_w \omega \rho_s + 2c\rho\sigma_{rad,w})} - \frac{64\pi c^5 n_w \rho^3 \sigma_{rad,w}}{A\omega^2 \rho_s (\eta_w \omega \rho_s + 2c\rho\sigma_{rad,w})^2} + \frac{64\pi c^6 n_w \rho^4 \sigma_{rad,w}^2}{A\omega^2 \rho_s (\eta_w \omega \rho_s + 2c\rho\sigma_{rad,w})^3} \tag{30b}$$

$$\frac{\partial \tau_w}{\partial n_w} = \frac{8\pi c^4 \rho^2 \sigma_{rad,w}^2}{A\omega^2 \rho_s (\eta_w \omega \rho_s + 2c\rho\sigma_{rad,w})} \tag{30c}$$

$$\frac{\partial^2 \tau_w}{\partial n_w^2} = 0 \tag{30d}$$

$$\frac{\partial \tau_w}{\partial \eta_w} = -\frac{8\pi c^4 n_w \rho^2 \sigma_{rad,w}^2}{A\omega(\eta_w \omega \rho_s + 2c\rho\sigma_{rad,w})^2} \tag{30e}$$

$$\frac{\partial^2 \tau_w}{\partial \eta_w^2} = \frac{16\pi c^4 n_w \rho^2 \rho_s \sigma_{rad,w}^2}{(A\eta_w \omega \rho_s + 2c\rho\sigma_{rad,w})^3} \tag{30f}$$

$$\frac{\partial \tau_w}{\partial \rho_s} = -\frac{8\pi c^4 n_w \rho^2 \sigma_{rad,w}^2}{A\omega^2 \rho_s^2 (\eta_w \omega \rho_s + 2c\rho\sigma_{rad,w})} - \frac{8\pi c^4 \eta_w n_w \rho^2 \sigma_{rad,w}^2}{A\omega\rho_s (\eta_w \omega \rho_s + 2c\rho\sigma_{rad,w})^2} \tag{30g}$$

$$\frac{\partial^2 \tau_w}{\partial \rho_s^2} = \frac{16\pi c^4 \eta_w^2 n_w \rho^2 \sigma_{rad,w}^2}{A\rho_s (\eta_w \omega \rho_s + 2c\rho\sigma_{rad,w})^3} + \frac{16\pi c^4 n_w \rho^2 \sigma_{rad,w}^2}{A\omega^2 \rho_s^3 (\eta_w \omega \rho_s + 2c\rho\sigma_{rad,w})} + \frac{16\pi c^4 \eta_w n_w \rho^2 \sigma_{rad,w}^2}{A\omega\rho_s^2 (\eta_w \omega \rho_s + 2c\rho\sigma_{rad,w})^2} \tag{30h}$$

All the necessary quantities have by now been computed from the considerations introduced above and the resonant acoustic transmission sensitivity can thus be evaluated in Eq.29.

3.7. Sensitivity of the nonresonant acoustic transmission

Nonresonant acoustic transmission is induced by the structural/acoustic coupling of mass controlled (low frequency) and stiffness controlled (high frequency) modes having a resonance frequency outside the considered band. Mass controlled modes can actually induce a significant amount of acoustic transmission and are considered within the analysis through Eq.15. It is evident that $\tau_{nr}(\omega)$ as expressed in Eq.15 is insensitive to all structural design parameters except the surface mass of the structure ρ_s. The only design parameters that have therefore the potential to

13

affect the nonresonant term are the layer thicknesses and densities of the composite structure. The parametric design sensitivities can therefore be written as

$$\frac{\partial \tau_{nr}(\omega)}{\partial \beta_i} = \frac{1}{\pi(\cos^2 \theta_{min} - \cos^2 \theta_{max})} \int_0^{2\pi} \int_0^{\theta_{max}} \frac{\partial \tau_{nr}(\theta, \phi, \omega)}{\partial \beta_i} \mathrm{d}\theta \mathrm{d}\phi \tag{31}$$

with the sensitivity of the directional transmission coefficient expressed as

$$\frac{\partial \tau_{nr}(\theta, \phi, \omega)}{\partial \beta_i} = \frac{\partial \tau_{nr}(\theta, \phi, \omega)}{\partial \rho_s} \frac{\partial \rho_s}{\partial \beta_i} = \frac{-8Z_0^2 \omega \sigma(\theta, \phi, \omega) \cos^2 \theta \sin \theta \mathrm{i}}{|2Z_0 + \rho_s \omega \mathrm{i}|^3} \frac{\partial \rho_s}{\partial \beta_i} \tag{32}$$

While for the second order sensitivity we have

$$\frac{\partial^2 \tau_{nr}(\omega)}{\partial \beta_j \partial \beta_i} = \frac{1}{\pi(\cos^2 \theta_{min} - \cos^2 \theta_{max})} \int_0^{2\pi} \int_0^{\theta_{max}} \frac{\partial^2 \tau_{nr}(\theta, \phi, \omega)}{\partial \rho_s^2} \frac{\partial \rho_s}{\partial \beta_j} \frac{\partial \rho_s}{\partial \beta_i} + \frac{\partial \tau_{nr}(\theta, \phi, \omega)}{\partial \rho_s} \frac{\partial^2 \rho_s}{\partial \beta_j \partial \beta_i} \mathrm{d}\theta \mathrm{d}\phi \tag{33}$$

with

$$\frac{\partial^2 \tau_{nr}(\theta, \phi, \omega)}{\partial \rho_s^2} = \frac{-24Z_0^2 \omega^2 \sigma(\theta, \phi, \omega) \cos^2 \theta \sin \theta}{|2Z_0 + \rho_s \omega \mathrm{i}|^4} \tag{34}$$

The computational cost of Eqs.31,33 is significantly reduced by the fact that the geometric radiation efficiency term $\sigma(\theta, \phi, \omega)$ is solely dependent on the area A of the considered structure which is not under investigation and is therefore computed only once in the optimization process. The quantity $|2Z_0 + \rho_s \omega \mathrm{i}|$ is therefore the only one that needs being recomputed for every design alteration. Given that $\rho_s = \sum_{l=l_1}^{l_{max}} \rho_{m,l} h_l$ with $\rho_{m,l}$ the mass density of layer l and h_l its thickness, it is straightforward to derive the quantities $\frac{\partial \rho_s}{\partial \beta_i} \frac{\partial \rho_s}{\partial \beta_j}$ and $\frac{\partial^2 \rho_s}{\partial \beta_i \partial \beta_j}$ for the composite panel.

4. Formulation of the optimization problem

The Newton's method will be hereby employed (ensuring quadratic convergence towards the solution) in order to optimise the considered set of parameters, which in the general orthotropic multilayer case can be expressed as

$$\mathbf{p} = \left\{ E_{x,1} E_{y,1} E_{z,1} v_{xy,1} v_{xz,1} v_{yz,1} G_{xy,1} G_{xz,1} G_{yz,1} h_1 \rho_{m,1} \cdots \rho_{m,l_{max}} \right\}^\top \tag{35}$$

with l_{max} the maximum number of layers. It is interesting to note that including η in an optimization procedure will not provide any helpful information, as $\delta\eta$ will not directly affect neither the mass, nor the stiffness of the panel. On the other hand it will always be beneficial for the reduction of τ_w, which suggests that a maximum η will always be the result of the computation. An effective way of including damping in the optimization process would be explicitly relating the increase of damping coefficient γ_l for layer l with the mass of the layer (e.g. accounting for the mass and damping increase implied by viscoleastic material inclusions).

The parameters may be considered to be constrained (e.g. $\beta_i \in [\beta_{i,min}, \beta_{i,max}]$). The objective function $\mathcal{F}(\mathbf{p})$ to be minimised is eventually to be decided. It is evident that the cost of added mass, as well as the one of static stiffness

14

loss should be included in $\mathcal{F}(\mathbf{p})$ (if not maximising the mass of the panel would be the evident solution for minimising the acoustic transmission). There is a number of cost criteria that can be applied to the stress-strain matrix coefficients [34] of a laminate in order to account for its axial, shear and flexural stiffness. A number of manufacturing related constraints (accounting for the realizability of the computed optimal design) can also be added to the optimization problem.

The cost function can eventually be expressed as

$$\mathcal{F}(\mathbf{p}) = \xi_3\tau^3(\mathbf{p}) + \xi_2\tau^2(\mathbf{p}) + \xi_1\tau(\mathbf{p}) + \xi_0 + \delta_3\rho_s^3(\mathbf{p}) + \delta_2\rho_s^2(\mathbf{p}) + \delta_1\rho_s(\mathbf{p}) + \delta_0 + \zeta_3 d_s^3(\mathbf{p}) + \zeta_2 d_s^2(\mathbf{p}) + \zeta_1 d_s(\mathbf{p}) + \zeta_0 \quad (36)$$

with τ, ρ_s and d_s being the acoustic, mass and stiffness performance indices respectively and ξ_i, δ_i, ζ_i coefficients that allow the designer to apply a polynomial curve fitting to the available cost data; thus facilitating the differentiability of $\mathcal{F}(\mathbf{p})$. Higher order polynomial or exponential fitting functions may be applied without loss of accuracy. The gradient vector of $\mathcal{F}(\mathbf{p})$ can therefore be computed as

$$\nabla\mathcal{F}(\mathbf{p}) = \left\{ \begin{array}{cccccccccccccc} \dfrac{\partial\mathcal{F}(\mathbf{p})}{\partial E_{x,1}} & \dfrac{\partial\mathcal{F}(\mathbf{p})}{\partial E_{y,1}} & \dfrac{\partial\mathcal{F}(\mathbf{p})}{\partial E_{z,1}} & \dfrac{\partial\mathcal{F}(\mathbf{p})}{\partial v_{xy,1}} & \dfrac{\partial\mathcal{F}(\mathbf{p})}{\partial v_{xz,1}} & \dfrac{\partial\mathcal{F}(\mathbf{p})}{\partial v_{yz,1}} & \dfrac{\partial\mathcal{F}(\mathbf{p})}{\partial G_{xy,1}} & \dfrac{\partial\mathcal{F}(\mathbf{p})}{\partial G_{xz,1}} & \dfrac{\partial\mathcal{F}(\mathbf{p})}{\partial G_{yz,1}} & \dfrac{\partial\mathcal{F}(\mathbf{p})}{\partial h_1} & \dfrac{\partial\mathcal{F}(\mathbf{p})}{\partial\rho_{m,1}} & \cdots & \dfrac{\partial\mathcal{F}(\mathbf{p})}{\partial\rho_{m,l_{max}}} \end{array} \right\}^\top \quad (37)$$

The derivatives of $\mathcal{F}(\mathbf{p})$ can be calculated using the chain rule (e.g. $\dfrac{\partial(\xi_3\tau^3)}{\partial\beta_i} = 3\xi_3\tau^2\dfrac{\partial\tau}{\partial\beta_i}$ and $\dfrac{\partial^2(\xi_3\tau^3)}{\partial\beta_j\partial\beta_i} = 6\xi_3\tau\dfrac{\partial\tau}{\partial\beta_j}\dfrac{\partial\tau}{\partial\beta_i} + 3\xi_3\tau^2\dfrac{\partial^2\tau}{\partial\beta_j\partial\beta_i}$). The Hessian matrix is subsequently formed using the computed second order sensitivity values

$$\mathbf{H} = \nabla^2\mathcal{F}(\mathbf{p}) = \begin{bmatrix}
\frac{\partial^2\mathcal{F}(\mathbf{p})}{\partial E_{x,1}^2} & \frac{\partial^2\mathcal{F}(\mathbf{p})}{\partial E_{x,1}\partial E_{y,1}} & \frac{\partial^2\mathcal{F}(\mathbf{p})}{\partial E_{x,1}\partial E_{z,1}} & \frac{\partial^2\mathcal{F}(\mathbf{p})}{\partial E_{x,1}\partial v_{xy,1}} & \frac{\partial^2\mathcal{F}(\mathbf{p})}{\partial E_{x,1}\partial v_{xz,1}} & \frac{\partial^2\mathcal{F}(\mathbf{p})}{\partial E_{x,1}\partial v_{yz,1}} & \frac{\partial^2\mathcal{F}(\mathbf{p})}{\partial E_{x,1}\partial G_{xy,1}} & \frac{\partial^2\mathcal{F}(\mathbf{p})}{\partial E_{x,1}\partial G_{xz,1}} & \frac{\partial^2\mathcal{F}(\mathbf{p})}{\partial E_{x,1}\partial G_{yz,1}} & \frac{\partial^2\mathcal{F}(\mathbf{p})}{\partial E_{x,1}\partial h_1} & \frac{\partial^2\mathcal{F}(\mathbf{p})}{\partial E_{x,1}\partial\rho_{m,1}} & \cdots & \frac{\partial^2\mathcal{F}(\mathbf{p})}{\partial E_{x,1}\partial\rho_{m,l_{max}}} \\
\frac{\partial^2\mathcal{F}(\mathbf{p})}{\partial E_{y,1}\partial E_{x,1}} & \frac{\partial^2\mathcal{F}(\mathbf{p})}{\partial E_{y,1}^2} & \frac{\partial^2\mathcal{F}(\mathbf{p})}{\partial E_{y,1}\partial E_{z,1}} & \frac{\partial^2\mathcal{F}(\mathbf{p})}{\partial E_{y,1}\partial v_{xy,1}} & \frac{\partial^2\mathcal{F}(\mathbf{p})}{\partial E_{y,1}\partial v_{xz,1}} & \frac{\partial^2\mathcal{F}(\mathbf{p})}{\partial E_{y,1}\partial v_{yz,1}} & \frac{\partial^2\mathcal{F}(\mathbf{p})}{\partial E_{y,1}\partial G_{xy,1}} & \frac{\partial^2\mathcal{F}(\mathbf{p})}{\partial E_{y,1}\partial G_{xz,1}} & \frac{\partial^2\mathcal{F}(\mathbf{p})}{\partial E_{y,1}\partial G_{yz,1}} & \frac{\partial^2\mathcal{F}(\mathbf{p})}{\partial E_{y,1}\partial h_1} & \frac{\partial^2\mathcal{F}(\mathbf{p})}{\partial E_{y,1}\partial\rho_{m,1}} & \cdots & \frac{\partial^2\mathcal{F}(\mathbf{p})}{\partial E_{y,1}\partial\rho_{m,l_{max}}} \\
\frac{\partial^2\mathcal{F}(\mathbf{p})}{\partial E_{z,1}\partial E_{x,1}} & \frac{\partial^2\mathcal{F}(\mathbf{p})}{\partial E_{z,1}\partial E_{y,1}} & \frac{\partial^2\mathcal{F}(\mathbf{p})}{\partial E_{z,1}^2} & \frac{\partial^2\mathcal{F}(\mathbf{p})}{\partial E_{z,1}\partial v_{xy,1}} & \frac{\partial^2\mathcal{F}(\mathbf{p})}{\partial E_{z,1}\partial v_{xz,1}} & \frac{\partial^2\mathcal{F}(\mathbf{p})}{\partial E_{z,1}\partial v_{yz,1}} & \frac{\partial^2\mathcal{F}(\mathbf{p})}{\partial E_{z,1}\partial G_{xy,1}} & \frac{\partial^2\mathcal{F}(\mathbf{p})}{\partial E_{z,1}\partial G_{xz,1}} & \frac{\partial^2\mathcal{F}(\mathbf{p})}{\partial E_{z,1}\partial G_{yz,1}} & \frac{\partial^2\mathcal{F}(\mathbf{p})}{\partial E_{z,1}\partial h_1} & \frac{\partial^2\mathcal{F}(\mathbf{p})}{\partial E_{z,1}\partial\rho_{m,1}} & \cdots & \frac{\partial^2\mathcal{F}(\mathbf{p})}{\partial E_{z,1}\partial\rho_{m,l_{max}}} \\
\frac{\partial^2\mathcal{F}(\mathbf{p})}{\partial v_{xy,1}\partial E_{x,1}} & \frac{\partial^2\mathcal{F}(\mathbf{p})}{\partial v_{xy,1}\partial E_{y,1}} & \frac{\partial^2\mathcal{F}(\mathbf{p})}{\partial v_{xy,1}\partial E_{z,1}} & \frac{\partial^2\mathcal{F}(\mathbf{p})}{\partial v_{xy,1}^2} & \frac{\partial^2\mathcal{F}(\mathbf{p})}{\partial v_{xy,1}\partial v_{xz,1}} & \frac{\partial^2\mathcal{F}(\mathbf{p})}{\partial v_{xy,1}\partial v_{yz,1}} & \frac{\partial^2\mathcal{F}(\mathbf{p})}{\partial v_{xy,1}\partial G_{xy,1}} & \frac{\partial^2\mathcal{F}(\mathbf{p})}{\partial v_{xy,1}\partial G_{xz,1}} & \frac{\partial^2\mathcal{F}(\mathbf{p})}{\partial v_{xy,1}\partial G_{yz,1}} & \frac{\partial^2\mathcal{F}(\mathbf{p})}{\partial v_{xy,1}\partial h_1} & \frac{\partial^2\mathcal{F}(\mathbf{p})}{\partial v_{xy,1}\partial\rho_{m,1}} & \cdots & \frac{\partial^2\mathcal{F}(\mathbf{p})}{\partial v_{xy,1}\partial\rho_{m,l_{max}}} \\
\frac{\partial^2\mathcal{F}(\mathbf{p})}{\partial v_{xz,1}\partial E_{x,1}} & \frac{\partial^2\mathcal{F}(\mathbf{p})}{\partial v_{xz,1}\partial E_{y,1}} & \frac{\partial^2\mathcal{F}(\mathbf{p})}{\partial v_{xz,1}\partial E_{z,1}} & \frac{\partial^2\mathcal{F}(\mathbf{p})}{\partial v_{xz,1}\partial v_{xy,1}} & \frac{\partial^2\mathcal{F}(\mathbf{p})}{\partial v_{xz,1}^2} & \frac{\partial^2\mathcal{F}(\mathbf{p})}{\partial v_{xz,1}\partial v_{yz,1}} & \frac{\partial^2\mathcal{F}(\mathbf{p})}{\partial v_{xz,1}\partial G_{xy,1}} & \frac{\partial^2\mathcal{F}(\mathbf{p})}{\partial v_{xz,1}\partial G_{xz,1}} & \frac{\partial^2\mathcal{F}(\mathbf{p})}{\partial v_{xz,1}\partial G_{yz,1}} & \frac{\partial^2\mathcal{F}(\mathbf{p})}{\partial v_{xz,1}\partial h_1} & \frac{\partial^2\mathcal{F}(\mathbf{p})}{\partial v_{xz,1}\partial\rho_{m,1}} & \cdots & \frac{\partial^2\mathcal{F}(\mathbf{p})}{\partial v_{xz,1}\partial\rho_{m,l_{max}}} \\
\frac{\partial^2\mathcal{F}(\mathbf{p})}{\partial v_{yz,1}\partial E_{x,1}} & \frac{\partial^2\mathcal{F}(\mathbf{p})}{\partial v_{yz,1}\partial E_{y,1}} & \frac{\partial^2\mathcal{F}(\mathbf{p})}{\partial v_{yz,1}\partial E_{z,1}} & \frac{\partial^2\mathcal{F}(\mathbf{p})}{\partial v_{yz,1}\partial v_{xy,1}} & \frac{\partial^2\mathcal{F}(\mathbf{p})}{\partial v_{yz,1}\partial v_{xz,1}} & \frac{\partial^2\mathcal{F}(\mathbf{p})}{\partial v_{yz,1}^2} & \frac{\partial^2\mathcal{F}(\mathbf{p})}{\partial v_{yz,1}\partial G_{xy,1}} & \frac{\partial^2\mathcal{F}(\mathbf{p})}{\partial v_{yz,1}\partial G_{xz,1}} & \frac{\partial^2\mathcal{F}(\mathbf{p})}{\partial v_{yz,1}\partial G_{yz,1}} & \frac{\partial^2\mathcal{F}(\mathbf{p})}{\partial v_{yz,1}\partial h_1} & \frac{\partial^2\mathcal{F}(\mathbf{p})}{\partial v_{yz,1}\partial\rho_{m,1}} & \cdots & \frac{\partial^2\mathcal{F}(\mathbf{p})}{\partial v_{yz,1}\partial\rho_{m,l_{max}}} \\
\frac{\partial^2\mathcal{F}(\mathbf{p})}{\partial G_{xy,1}\partial E_{x,1}} & \frac{\partial^2\mathcal{F}(\mathbf{p})}{\partial G_{xy,1}\partial E_{y,1}} & \frac{\partial^2\mathcal{F}(\mathbf{p})}{\partial G_{xy,1}\partial E_{z,1}} & \frac{\partial^2\mathcal{F}(\mathbf{p})}{\partial G_{xy,1}\partial v_{xy,1}} & \frac{\partial^2\mathcal{F}(\mathbf{p})}{\partial G_{xy,1}\partial v_{xz,1}} & \frac{\partial^2\mathcal{F}(\mathbf{p})}{\partial G_{xy,1}\partial v_{yz,1}} & \frac{\partial^2\mathcal{F}(\mathbf{p})}{\partial G_{xy,1}^2} & \frac{\partial^2\mathcal{F}(\mathbf{p})}{\partial G_{xy,1}\partial G_{xz,1}} & \frac{\partial^2\mathcal{F}(\mathbf{p})}{\partial G_{xy,1}\partial G_{yz,1}} & \frac{\partial^2\mathcal{F}(\mathbf{p})}{\partial G_{xy,1}\partial h_1} & \frac{\partial^2\mathcal{F}(\mathbf{p})}{\partial G_{xy,1}\partial\rho_{m,1}} & \cdots & \frac{\partial^2\mathcal{F}(\mathbf{p})}{\partial G_{xy,1}\partial\rho_{m,l_{max}}} \\
\frac{\partial^2\mathcal{F}(\mathbf{p})}{\partial G_{xz,1}\partial E_{x,1}} & \frac{\partial^2\mathcal{F}(\mathbf{p})}{\partial G_{xz,1}\partial E_{y,1}} & \frac{\partial^2\mathcal{F}(\mathbf{p})}{\partial G_{xz,1}\partial E_{z,1}} & \frac{\partial^2\mathcal{F}(\mathbf{p})}{\partial G_{xz,1}\partial v_{xy,1}} & \frac{\partial^2\mathcal{F}(\mathbf{p})}{\partial G_{xz,1}\partial v_{xz,1}} & \frac{\partial^2\mathcal{F}(\mathbf{p})}{\partial G_{xz,1}\partial v_{yz,1}} & \frac{\partial^2\mathcal{F}(\mathbf{p})}{\partial G_{xz,1}\partial G_{xy,1}} & \frac{\partial^2\mathcal{F}(\mathbf{p})}{\partial G_{xz,1}^2} & \frac{\partial^2\mathcal{F}(\mathbf{p})}{\partial G_{xz,1}\partial G_{yz,1}} & \frac{\partial^2\mathcal{F}(\mathbf{p})}{\partial G_{xz,1}\partial h_1} & \frac{\partial^2\mathcal{F}(\mathbf{p})}{\partial G_{xz,1}\partial\rho_{m,1}} & \cdots & \frac{\partial^2\mathcal{F}(\mathbf{p})}{\partial G_{xz,1}\partial\rho_{m,l_{max}}} \\
\frac{\partial^2\mathcal{F}(\mathbf{p})}{\partial G_{yz,1}\partial E_{x,1}} & \frac{\partial^2\mathcal{F}(\mathbf{p})}{\partial G_{yz,1}\partial E_{y,1}} & \frac{\partial^2\mathcal{F}(\mathbf{p})}{\partial G_{yz,1}\partial E_{z,1}} & \frac{\partial^2\mathcal{F}(\mathbf{p})}{\partial G_{yz,1}\partial v_{xy,1}} & \frac{\partial^2\mathcal{F}(\mathbf{p})}{\partial G_{yz,1}\partial v_{xz,1}} & \frac{\partial^2\mathcal{F}(\mathbf{p})}{\partial G_{yz,1}\partial v_{yz,1}} & \frac{\partial^2\mathcal{F}(\mathbf{p})}{\partial G_{yz,1}\partial G_{xy,1}} & \frac{\partial^2\mathcal{F}(\mathbf{p})}{\partial G_{yz,1}\partial G_{xz,1}} & \frac{\partial^2\mathcal{F}(\mathbf{p})}{\partial G_{yz,1}^2} & \frac{\partial^2\mathcal{F}(\mathbf{p})}{\partial G_{yz,1}\partial h_1} & \frac{\partial^2\mathcal{F}(\mathbf{p})}{\partial G_{yz,1}\partial\rho_{m,1}} & \cdots & \frac{\partial^2\mathcal{F}(\mathbf{p})}{\partial G_{yz,1}\partial\rho_{m,l_{max}}} \\
\frac{\partial^2\mathcal{F}(\mathbf{p})}{\partial h_1\partial E_{x,1}} & \frac{\partial^2\mathcal{F}(\mathbf{p})}{\partial h_1\partial E_{y,1}} & \frac{\partial^2\mathcal{F}(\mathbf{p})}{\partial h_1\partial E_{z,1}} & \frac{\partial^2\mathcal{F}(\mathbf{p})}{\partial h_1\partial v_{xy,1}} & \frac{\partial^2\mathcal{F}(\mathbf{p})}{\partial h_1\partial v_{xz,1}} & \frac{\partial^2\mathcal{F}(\mathbf{p})}{\partial h_1\partial v_{yz,1}} & \frac{\partial^2\mathcal{F}(\mathbf{p})}{\partial h_1\partial G_{xy,1}} & \frac{\partial^2\mathcal{F}(\mathbf{p})}{\partial h_1\partial G_{xz,1}} & \frac{\partial^2\mathcal{F}(\mathbf{p})}{\partial h_1\partial G_{yz,1}} & \frac{\partial^2\mathcal{F}(\mathbf{p})}{\partial h_1^2} & \frac{\partial^2\mathcal{F}(\mathbf{p})}{\partial h_1\partial\rho_{m,1}} & \cdots & \frac{\partial^2\mathcal{F}(\mathbf{p})}{\partial h_1\partial\rho_{m,l_{max}}} \\
\frac{\partial^2\mathcal{F}(\mathbf{p})}{\partial\rho_{m,1}\partial E_{x,1}} & \frac{\partial^2\mathcal{F}(\mathbf{p})}{\partial\rho_{m,1}\partial E_{y,1}} & \frac{\partial^2\mathcal{F}(\mathbf{p})}{\partial\rho_{m,1}\partial E_{z,1}} & \frac{\partial^2\mathcal{F}(\mathbf{p})}{\partial\rho_{m,1}\partial v_{xy,1}} & \frac{\partial^2\mathcal{F}(\mathbf{p})}{\partial\rho_{m,1}\partial v_{xz,1}} & \frac{\partial^2\mathcal{F}(\mathbf{p})}{\partial\rho_{m,1}\partial v_{yz,1}} & \frac{\partial^2\mathcal{F}(\mathbf{p})}{\partial\rho_{m,1}\partial G_{xy,1}} & \frac{\partial^2\mathcal{F}(\mathbf{p})}{\partial\rho_{m,1}\partial G_{xz,1}} & \frac{\partial^2\mathcal{F}(\mathbf{p})}{\partial\rho_{m,1}\partial G_{yz,1}} & \frac{\partial^2\mathcal{F}(\mathbf{p})}{\partial\rho_{m,1}\partial h_1} & \frac{\partial^2\mathcal{F}(\mathbf{p})}{\partial\rho_{m,1}^2} & \cdots & \frac{\partial^2\mathcal{F}(\mathbf{p})}{\partial\rho_{m,1}\partial\rho_{m,l_{max}}} \\
\cdots & \cdots & \cdots & \cdots & \cdots & \cdots & \cdots & \cdots & \cdots & \cdots & \cdots & \cdots & \cdots \\
\frac{\partial^2\mathcal{F}(\mathbf{p})}{\partial\rho_{m,l_{max}}\partial E_{x,1}} & \frac{\partial^2\mathcal{F}(\mathbf{p})}{\partial\rho_{m,l_{max}}\partial E_{y,1}} & \frac{\partial^2\mathcal{F}(\mathbf{p})}{\partial\rho_{m,l_{max}}\partial E_{z,1}} & \frac{\partial^2\mathcal{F}(\mathbf{p})}{\partial\rho_{m,l_{max}}\partial v_{xy,1}} & \frac{\partial^2\mathcal{F}(\mathbf{p})}{\partial\rho_{m,l_{max}}\partial v_{xz,1}} & \frac{\partial^2\mathcal{F}(\mathbf{p})}{\partial\rho_{m,l_{max}}\partial v_{yz,1}} & \frac{\partial^2\mathcal{F}(\mathbf{p})}{\partial\rho_{m,l_{max}}\partial G_{xy,1}} & \frac{\partial^2\mathcal{F}(\mathbf{p})}{\partial\rho_{m,l_{max}}\partial G_{xz,1}} & \frac{\partial^2\mathcal{F}(\mathbf{p})}{\partial\rho_{m,l_{max}}\partial G_{yz,1}} & \frac{\partial^2\mathcal{F}(\mathbf{p})}{\partial\rho_{m,l_{max}}\partial h_1} & \frac{\partial^2\mathcal{F}(\mathbf{p})}{\partial\rho_{m,l_{max}}\partial\rho_{m,1}} & \cdots & \frac{\partial^2\mathcal{F}(\mathbf{p})}{\partial\rho_{m,l_{max}}^2}
\end{bmatrix}$$

$$(38)$$

A commercially embedded constrained nonlinear optimization algorithm [35] is eventually employed in order to compute the optimal parameter vector $\mathbf{p}$ that minimises $\mathcal{F}(\mathbf{p})$ at a certain frequency.

5. Numerical case studies

In order to validate the exhibited optimization approach, an asymmetric sandwich panel comprising two facesheets and a core is modelled in this section. The lower facesheet has a thickness h_1=1mm and is made of a material having $\rho_{m,1}$=3000e^{-9}kg/mm^3, E_1 = 70GPa and a Poisson's ration v_1=0.1. The upper facesheet has a thickness equal to h_3=2mm and is made of the same material as the lower facesheet. The core has a thickness h_2=10mm and is made of a material with $\rho_{m,2}$=50e^{-9}kg/mm^3, E_2 = 0.07GPa and v_2=0.4. Three FEs are used in the sense of thickness in order to model the structure. All computations were conducted using the R2013a version of MATLAB$^®$.

5.1. Results on the wave sensitivity analysis of a layered structure

In this section the sensitivity of the wave characteristics with respect to the mechanical and geometric characteristics of the sandwich panel are sought as discussed in Sec.2. The results are compared to a FD approach throughout this section. In order to implement the FD approach a perturbation of 0.1% was considered for each structural parameter. The resulting FD sensitivity can be computed by

$$\frac{\partial k}{\partial \beta} = \frac{k_p - k_0}{\beta_p - \beta_0} \tag{39}$$

with k_p the perturbed wavenumber value for β_p and k_0 the corresponding wavenumber for the unperturbed parameter β_0.

The sensitivity of the flexural wavenumber k with respect to the thickness of each facesheet layer is presented in Fig.3. It is particularly interesting to note that in the very low frequency range increasing the thickness of both facesheets will imply a softening effect to the structural behaviour, shifting the flexural wavenumbers upwards. This mainly suggests that the effect of the added mass overcomes the effect of added stiffness for both δh_1 and δh_3. However at higher frequencies the results change radically for the thicker upper facesheet, with δh_3 now shifting the wavenumbers to lower values, suggesting a stiffening phenomenon in the structural dynamic behaviour. An excellent agreement is observed between the presented approach and the FD method.

[Figure 3 about here.]

The sensitivity of k with respect to the thickness of the sandwich core layer is presented in Fig.4. A very interesting effect is that the influence of δh_2 on the flexural wavenumber becomes maximum for a certain frequency (approximately 2000 Hz), where the stiffening effect of δh_2 becomes maximum. An intense nonlinearity is observed in the relation of $\delta \omega$ to δk. A constant decrease of this influence is observed beyond that point. The stiffening effect is probably due to the greater separation of the two facesheets with δh_2. It is very probable however that for higher wavenumber values δh_c will have a softening effect on the flexural wavenumber with the depicted curve passing to positive values ok δk. This is the frequency range within which the two facesheets of the structure start vibrating independently of each other (see [36]) thus the core thickness has an insignificant impact on the flexural wave speed.

16

[Figure 4 about here.]

In Fig.5, the sensitivity of k with respect to the mass density of the sandwich facesheet layers is presented. As expected, both $\delta\rho_{m,1}$ and $\delta\rho_{m,3}$ will shift the wavenumber curve to higher values, suggesting a softening phenomenon. This effect will be greater for the thicker upper facesheet at low k values. A highly nonlinear behaviour is again observed and it is interesting to see that there is a critical frequency value at which the effect of $\delta\rho_{m,1}$ and $\delta\rho_{m,3}$ will be the same. Beyond this critical wavenumber the softening effect will paradoxically be more intense for $\delta\rho_{m,1}$.

[Figure 5 about here.]

The perturbation of k with respect to v_2 for the sandwich core is presented in Fig.6. The effect of δv_2 is softening up to a certain wavenumber value, beyond which an intense decrease of the sensitivity is observed which stiffens the flexural structural behaviour.

[Figure 6 about here.]

5.2. Results on the SEA sensitivity analysis of a layered structure

In this section the sensitivity of the SEA quantities, namely the modal density, the radiation efficiency and the damping loss factor are computed as discussed in Sec.3 and evaluated.

The first order sensitivity of the modal density of the composite panel with regard to the layer thicknesses and Young's moduli are exhibited in Figs.7,8 respectively. In Fig.8 all sensitivity values are negative, it was thus preferred to present the absolute result values in order to employ a clearer logarithmic scale. It can be observed that the stiffening effect induced by δh_3 in the high frequency range, also induces a high reduction of the modal density, while a maximum softening effect is observed for both δh_1, δh_3 in the low frequency range (approximately 1000 Hz). With regard to the effect of the Young's modulus it is observed that its increase can imply more drastic hardening effects for the core layer compared to the one of the facesheets.

[Figure 7 about here.]

[Figure 8 about here.]

The sensitivity of the acoustic radiation efficiency for the composite panel with regard to the layer thicknesses is presented in Fig.9. In order to use a clearer logarithmic scale the quantity $\delta 10\log(\sigma)/\delta h$ is plotted. It is generally observed that altering the thickness of the thicker facesheet h_3 will have a maximum effect on the radiation efficiency, while the opposite is true for altering the thickness of the core layer. The maximum impact on σ is as expected observed around the acoustic coincidence frequency (approximately 5800 Hz in this case study). It is interesting to note that the effect of δh_1 will have an opposite effect on σ compared to δh_3.

The same quantity is presented in Fig.10, this time as a function of the mass densities of the three layers. This time the effect of $\delta\rho_{m,2}$ will have a maximum impact on the acoustic radiation efficiency (probably due to the higher volume of the core layer), again around the acoustic coincidence frequency.

17

[Figure 9 about here.]

[Figure 10 about here.]

The sensitivity of the loss factor η for the flexural wave is subsequently discussed. Its first order sensitivity with regard to the layer thicknesses is exhibited in Fig.11. It is evident that the maximum impact of δh_i on the total loss factor of the panel takes place in the low frequency range. For higher frequencies it can be observed that $\delta\eta/\delta h_1$ converges to a constant value, while the increase of the core thickness has a continuously diminishing impact on η.

In Fig.12 the same quantity is presented, this time as a function of the individual damping coefficient of each layer γ_i. Throughout the entire frequency range it is observed that increasing the damping coefficient of the core layer $\delta\gamma_2$ will have a maximum effect on the total loss factor of the panel. It is observed that the effect of $\delta\gamma_i$ on the total loss factor is diminishing with frequency.

[Figure 11 about here.]

[Figure 12 about here.]

The impact of the structural parameters on the acoustic transmission coefficient and the STL of the composite structure is eventually computed. In Fig.13 the sensitivity of the structure's TL with regard to the layer thicknesses is presented. It is evident that altering the thickness of the upper thicker layer will induce the maximum effect on TL, especially close to the acoustic coincidence region. On the other hand, altering the core thickness will have an insignificant effect on the TL index.

[Figure 13 about here.]

In Fig.14 the sensitivity of the TL with regard to the layer mass densities is presented. It is evident that the results follow the trend of the ones shown for the radiation efficiency of the panel in Fig.10 with the mass density of the core layer being the one that influences the TL the most.

[Figure 14 about here.]

The same result is exhibited in Fig.15, this time regarding the sensitivity with respect to the Young's moduli of the layers. Once again it is observed that altering the Young's modulus of the core can have the most significant impact, while the influence of δE_1 and δE_3 are generally insignificant.

[Figure 15 about here.]

5.3. Structural design optimization of the layered structure

As discussed in Sec.4, the criteria to be considered within the optimization process of the mechanical and geometric characteristics of the panel are its mass, stiffness and vibroacoustic performance. The surface mass of the panel ρ_s is chosen as a representative mass index, the total acoustic transmission coefficient τ is selected as the vibroacoustic performance index, while with regard to the structural stiffness and for the sake of simplicity we will hereby assume that we are solely interested in the sum of the static flexural stiffnesses of the panel D_{xx}, D_{yy} expressed as

$$d_s = D_{xx} + D_{yy} = \frac{1}{3} \sum_{l=l_1}^{l_{max}} \left((Q_{xx,l} + Q_{yy,l})(z_l^3 - z_{l-1}^3) \right) \tag{40a}$$

$$Q_{xx,l} = E_{x,l} \frac{1 - v_{yz,l}^2}{\Delta_l} \tag{40b}$$

$$Q_{yy,l} = E_{y,l} \frac{1 - v_{xz,l}^2}{\Delta_l} \tag{40c}$$

$$\Delta_l = 1 - v_{xy,l}^2 - v_{yz,l}^2 - v_{zx,l}^2 - 2v_{xy,l}v_{yz,l}v_{zx,l} \tag{40d}$$

which in the case of an isotropic composite panel gives

$$d_s = \frac{2}{3} \sum_{l=l_1}^{l_{max}} \left(Q_l(z_l^3 - z_{l-1}^3) \right) \tag{41}$$

with z_l the coordinate of the upper surface of layer l in the thickness direction. The design cost functions, employed in order to decide the relation between ρ_s, τ and d_s and the corresponding induced design cost are exhibited in Fig.16 and eventually result in the objective function

$$\mathcal{F}(\mathbf{p}) = 4.000\mathrm{e}^8\tau^3(\mathbf{p}) + 2.920\mathrm{e}^6\tau^2(\mathbf{p}) - 6.245\tau(\mathbf{p}) + 3.005 + 1.332\mathrm{e}^{15}\rho_s^3(\mathbf{p}) + 6.940\mathrm{e}^{10}\rho_s^2(\mathbf{p}) - \tag{42a}$$

$$7.512\mathrm{e}^5\rho_s(\mathbf{p}) + 1.873 - 9.369\mathrm{e}^{-31}d_s^3(\mathbf{p}) + 1.405\mathrm{e}^{-19}d_s^2(\mathbf{p}) - 3.816\mathrm{e}^{-9}d_s(\mathbf{p}) + 29.936$$

to be minimised. It is noted that other polynomial as well as exponential fitting functions can be employed without loss of accuracy. The following constraints are considered for the optimization procedure

[Figure 16 about here.]

$E_1 \in [40\mathrm{GPa},110\mathrm{GPa}]$, $v_1 \in [0.05,0.30]$, $h_1 \in [0.2\mathrm{mm},3\mathrm{mm}]$, $\rho_{m,1} \in [1500\mathrm{kg/m}^3,4500\mathrm{kg/m}^3]$

$E_2 \in [40\mathrm{MPa},110\mathrm{MPa}]$, $v_2 \in [0.05,0.49]$, $h_2 \in [5\mathrm{mm},20\mathrm{mm}]$, $\rho_{m,2} \in [10\mathrm{kg/m}^3,150\mathrm{kg/m}^3]$

$E_3 \in [40\mathrm{GPa},110\mathrm{GPa}]$, $v_3 \in [0.05,0.30]$, $h_3 \in [0.2\mathrm{mm},4\mathrm{mm}]$, $\rho_{m,3} \in [1500\mathrm{kg/m}^3,4500\mathrm{kg/m}^3]$

Additional constraints (e.g. minimum axial and/or flexural stiffness, maximum surface mass e.t.c) can be considered. The constrained optimization problem is implemented within MATLAB and the nonlinear optimization algorithm *fmincon* (see [35]) is employed in order to compute the optimal parameter vector $\mathbf{p}$ that minimises $\mathcal{F}(\mathbf{p})$.

5.4. Optimal parameters and discussion on the computational efficiency

The optimization problem is solved for $k = 0.13$rad/mm, and the optimal material and geometric parameters that minimise the cost function presented in Eq.42 are computed as follows

$$E_1 = 80.9\text{GPa}, \; v_1 = 0.12, \; h_1 = 1.19\text{mm}, \; \rho_{m,1} = 1647\text{kg/m}^3$$

$$E_2 = 110\text{MPa}, \; v_2 = 0.37, \; h_2 = 10.53\text{mm}, \; \rho_{m,2} = 14.6\text{kg/m}^3$$

$$E_3 = 58.3\text{GPa}, \; v_3 = 0.19, \; h_3 = 1.74\text{mm}, \; \rho_{m,3} = 1500\text{kg/m}^3$$

It is noted that the only quantities laying on the limits of the predefined constraints which could potentially further improve the overall structural performance are the Young's modulus of the core layer E_2 as well as the mass density of the upper layer $\rho_{m,3}$. Optimising the structure in a broadband frequency range can be done by averaging the optimal parameters over the frequency range of interest or by introducing a weighting average for the frequency bands that are considered more important (e.g. frequency range corresponding to the external acoustic excitation). The optimization process was completed in 8 iterations each of which lasted approximately 78 seconds, resulting in a total computation time of 630s. This suggests that a broadband structural optimization is feasible within a few hours, even on a conventional computing equipment.

6. Conclusions

In this work, the optimal mechanical and geometric characteristics for layered composite structures subject to vibroacoustic excitations were derived in a wave SEA context. The main conclusions of the paper are summarised as:

(i) The formulation of the symbolic expression of the stiffness and mass matrices for a linear solid FE were presented. These formulations can be used in order to derive the symbolic global matrices of the modelled segment, as well as the sensitivity of the global matrices with regard to any structural parameter. Non conservative structural systems are also modelled by the exhibited approach.

(ii) An intense frequency dependent variation of the sensitivity of the propagating wave characteristics has been observed as a function of the design of the composite structure. This also implies frequency dependence of the optimal design parameters.

(iii) Expressions for the first and second order sensitivities of the SEA quantities, namely the modal density, the radiation efficiency and the damping loss factor of the composite panel were derived. The design parametric sensitivity for each of the SEA quantities, as well as of the acoustic transmission coefficient were found to be highly frequency dependent. The impact of the design alteration on the vibroacoustic response was found to be maximum in the vicinity of the acoustic coincidence range for most parameters.

(iv) The suggested optimization process is computationally efficient, allowing for a broadband structural design optimization of a layered structure in a rational period of time, even with the use of conventional computing equipment.

References

[1] D. J. Mead, A general theory of harmonic wave propagation in linear periodic systems with multiple coupling, Journal of Sound and Vibration 27 (1973) 235–60.

[2] R. Langley, A note on the force boundary conditions for two-dimensional periodic structures with corner freedoms, Journal of Sound and Vibration 167 (1993) 377–81.

[3] B. R. Mace, D. Duhamel, M. J. Brennan, L. Hinke, Finite element prediction of wave motion in structural waveguides, The Journal of the Acoustical Society of America 117 (2005) 2835–43.

[4] J.-M. Mencik, M. Ichchou, Multi-mode propagation and diffusion in structures through finite elements, European Journal of Mechanics-A/Solids 24 (2005) 877–98.

[5] G. Maidanik, Response of ribbed panels to reverberant acoustic fields, the Journal of the Acoustical Society of America 34 (1962) 809–26.

[6] C. Wallace, Radiation resistance of a rectangular panel, The Journal of the Acoustical Society of America 51 (1972) 946–52.

[7] R. Lyon, Statistical energy analysis of dynamical systems: theory and applications, MIT press Cambridge, 1975.

[8] F. G. Leppington, E. G. Broadbent, K. H. Heron, Acoustic radiation efficiency of rectangular panels, in: Proceedings of The Royal Society of London, Series A: Mathematical and Physical Sciences, volume 382, pp. 245–71.

[9] S. Ghinet, N. Atalla, H. Osman, The transmission loss of curved laminates and sandwich composite panels, The Journal of the Acoustical Society of America 118 (2005) 774–90.

[10] V. Cotoni, R. S. Langley, P. J. Shorter, A statistical energy analysis subsystem formulation using finite element and periodic structure theory, Journal of Sound and Vibration 318 (2008) 1077–108.

[11] D. Chronopoulos, M. Ichchou, B. Troclet, O. Bareille, Computing the broadband vibroacoustic response of arbitrarily thick layered panels by a wave finite element approach, Applied Acoustics 77 (2014) 89–98.

[12] D. Chronopoulos, B. Troclet, M. Ichchou, J. Lainé, A unified approach for the broadband vibroacoustic response of composite shells, Composites Part B: Engineering 43 (2012) 1837–46.

[13] R. B. Nelson, Simplified calculation of eigenvector derivatives, AIAA journal 14 (1976) 1201–5.

[14] R. T. Haftka, H. M. Adelman, Recent developments in structural sensitivity analysis, Structural optimization 1 (1989) 137–51.

[15] S. Adhikari, M. I. Friswell, Eigenderivative analysis of asymmetric non-conservative systems, International Journal for Numerical Methods in Engineering 51 (2001) 709–33.

[16] K. K. Choi, N.-H. Kim, Structural sensitivity analysis and optimization 1: linear systems, volume 1, Springer, 2006.

[17] K. Sobczyk, Stochastic wave propagation, Elsevier, 1985.

[18] A. Belyaev, Comparative study of various approaches to stochastic elastic wave propagation, Acta mechanica 125 (1997) 3–16.

[19] K. Koo, B. Pluymers, W. Desmet, S. Wang, Vibro-acoustic design sensitivity analysis using the wave-based method, Journal of Sound and Vibration 330 (2011) 4340–51.

[20] M. Ruzzene, F. Scarpa, Directional and band-gap behavior of periodic auxetic lattices, physica status solidi (b) 242 (2005) 665–80.

[21] M. Ichchou, F. Bouchoucha, M. Ben Souf, O. Dessombz, M. Haddar, Stochastic wave finite element for random periodic media through first-order perturbation, Computer Methods in Applied Mechanics and Engineering 200 (2011) 2805–13.

[22] B. Souf, O. Bareille, M. Ichchou, F. Bouchoucha, M. Haddar, Waves and energy in random elastic guided media through the stochastic wave finite element method, Physics Letters A 377 (2013) 2255–64.

[23] R. Le Riche, R. T. Haftka, Optimization of laminate stacking sequence for buckling load maximization by genetic algorithm, AIAA journal 31 (1993) 951–6.

[24] M. Walker, R. E. Smith, A technique for the multiobjective optimisation of laminated composite structures using genetic algorithms and finite element analysis, Composite Structures 62 (2003) 123–8.

[25] S. Omkar, D. Mudigere, G. N. Naik, S. Gopalakrishnan, Vector evaluated particle swarm optimization (vepso) for multi-objective design optimization of composite structures, Computers & structures 86 (2008) 1–14.

[26] R. Langley, N. Bardell, P. Loasby, The optimal design of near-periodic structures to minimize vibration transmission and stress levels, Journal of Sound and Vibration 207 (1997) 627–46.

[27] M. I. Hussein, G. M. Hulbert, R. A. Scott, Dispersive elastodynamics of 1d banded materials and structures: analysis, Journal of sound and vibration 289 (2006) 779–806.

[28] M. I. Hussein, K. Hamza, G. M. Hulbert, R. A. Scott, K. Saitou, Multiobjective evolutionary optimization of periodic layered materials for desired wave dispersion characteristics, Structural and Multidisciplinary Optimization 31 (2006) 60–75.

[29] M. Collet, K. A. Cunefare, M. N. Ichchou, Wave motion optimization in periodically distributed shunted piezocomposite beam structures, Journal of Intelligent Material Systems and Structures (2008).

[30] J. Allard, N. Atalla, Propagation of Sound in Porous Media: Modelling Sound Absorbing Materials 2e, John Wiley & Sons, 2009.

[31] R. Courant, D. Hilbert, Methoden der mathematischen Physik, vol. 1, volume 2, Berlin, 1931.

[32] J. G. McDaniel, P. Dupont, L. Salvino, A wave approach to estimating frequency-dependent damping under transient loading, Journal of sound and vibration 231 (2000) 433–49.

[33] E. Manconi, B. R. Mace, Estimation of the loss factor of viscoelastic laminated panels from finite element analysis, Journal of Sound and Vibration 329 (2010) 3928–39.

[34] R. M. Jones, Mechanics of composite materials, CRC Press, 1998.

[35] A. Grace, M. Works, Optimization Toolbox: For Use with MATLAB: User's Guide, Math works, 1990.

[36] G. Kurtze, B. Watters, New wall design for high transmission loss or high damping, The Journal of the Acoustical Society of America 31 (1959) 739–48.

[37] C. A. Felippa, R. W. Clough, The finite element method in solid mechanics, American Mathematical Society, 1970.

Appendix A. Sensitivity analysis of a solid FE

A linear solid FE is hereby considered as shown in Fig.17.

[Figure 17 about here.]

Following the isoparametric notation introduced in [37] the geometry of the element is described as

$$
\left\{ \begin{array}{c} x \\ y \\ z \end{array} \right\} = \left[\begin{array}{cccccccc} x_1 & x_2 & x_3 & x_4 & x_5 & x_6 & x_7 & x_8 \\ y_1 & y_2 & y_3 & y_4 & y_5 & y_6 & y_7 & y_8 \\ z_1 & z_2 & z_3 & z_4 & z_5 & z_6 & z_7 & z_8 \end{array} \right] \left\{ \begin{array}{c} N_1 \\ N_2 \\ N_3 \\ N_4 \\ N_5 \\ N_6 \\ N_7 \\ N_8 \end{array} \right\}
\tag{A.1}
$$

The displacement interpolations are expressed as

$$
\left\{
\begin{array}{c}
u_x \\
u_y \\
u_z
\end{array}
\right\}
=
\left[
\begin{array}{cccccccc}
u_{x1} & u_{x2} & u_{x3} & u_{x4} & u_{x5} & u_{x6} & u_{x7} & u_{x8} \\
u_{y1} & u_{y2} & u_{y3} & u_{y4} & u_{y5} & u_{y6} & u_{y7} & u_{y8} \\
u_{z1} & u_{z2} & u_{z3} & u_{z4} & u_{z5} & u_{z6} & u_{z7} & u_{z8}
\end{array}
\right]
\left\{
\begin{array}{c}
N_1 \\
N_2 \\
N_3 \\
N_4 \\
N_5 \\
N_6 \\
N_7 \\
N_8
\end{array}
\right\}
\tag{A.2}
$$

Linear shape functions are assumed for the element

$$
\begin{aligned}
N_1 &= \tfrac{1}{8}(1 - \xi)(1 - \eta)(1 + \mu) \\
N_2 &= \tfrac{1}{8}(1 - \xi)(1 - \eta)(1 - \mu) \\
N_3 &= \tfrac{1}{8}(1 - \xi)(1 + \eta)(1 - \mu) \\
N_4 &= \tfrac{1}{8}(1 - \xi)(1 + \eta)(1 + \mu) \\
N_5 &= \tfrac{1}{8}(1 + \xi)(1 - \eta)(1 + \mu) \\
N_6 &= \tfrac{1}{8}(1 + \xi)(1 - \eta)(1 - \mu) \\
N_7 &= \tfrac{1}{8}(1 + \xi)(1 + \eta)(1 - \mu) \\
N_8 &= \tfrac{1}{8}(1 + \xi)(1 + \eta)(1 + \mu)
\end{aligned}
\tag{A.3}
$$

The element stiffness matrix $\mathbf{k}$ is formally given by the volume integral

$$
\mathbf{k} = \int_{-1}^{1} \int_{-1}^{1} \int_{-1}^{1} \mathbf{B}^\top \mathbf{D} \mathbf{B} |\mathbf{J}| \, \mathrm{d}\eta \mathrm{d}\xi \mathrm{d}\mu
\tag{A.4}
$$

while the element mass and damping matrices $\mathbf{m}$, $\mathbf{c}$ can be determined as

$$
\mathbf{m} = \int_{-1}^{1} \int_{-1}^{1} \int_{-1}^{1} \mathbf{N}^\top \rho_m \mathbf{N} |\mathbf{J}| \, \mathrm{d}\eta \mathrm{d}\xi \mathrm{d}\mu
\tag{A.5}
$$

$$
\mathbf{c} = \int_{-1}^{1} \int_{-1}^{1} \int_{-1}^{1} \mathbf{N}^\top \gamma \, \mathbf{N} |\mathbf{J}| \, \mathrm{d}\eta \mathrm{d}\xi \mathrm{d}\mu
\tag{A.6}
$$

with

$$
\mathbf{N} =
\left[
\begin{array}{ccccccc}
N_1 & 0 & 0 & \cdots & N_8 & 0 & 0 \\
0 & N_1 & 0 & \cdots & 0 & N_8 & 0 \\
0 & 0 & N_1 & \cdots & 0 & 0 & N_8
\end{array}
\right]
\tag{A.7}
$$

while ρ_m is the mass density of the material and γ the material damping coefficient. It is also noted that

$$\mathbf{B} = \begin{bmatrix} \frac{\partial N_1}{\partial x} & 0 & 0 & \frac{\partial N_2}{\partial x} & \cdots & \frac{\partial N_8}{\partial x} & 0 & 0 \\ 0 & \frac{\partial N_1}{\partial y} & 0 & 0 & \cdots & 0 & \frac{\partial N_8}{\partial y} & 0 \\ 0 & 0 & \frac{\partial N_1}{\partial z} & 0 & \cdots & 0 & 0 & \frac{\partial N_8}{\partial z} \\ \frac{\partial N_1}{\partial y} & \frac{\partial N_1}{\partial x} & 0 & \frac{\partial N_2}{\partial y} & \cdots & \frac{\partial N_8}{\partial y} & \frac{\partial N_8}{\partial x} & 0 \\ 0 & \frac{\partial N_1}{\partial z} & \frac{\partial N_1}{\partial y} & 0 & \cdots & 0 & \frac{\partial N_8}{\partial z} & \frac{\partial N_8}{\partial y} \\ \frac{\partial N_1}{\partial z} & 0 & \frac{\partial N_1}{\partial x} & \frac{\partial N_2}{\partial z} & \cdots & \frac{\partial N_8}{\partial z} & 0 & \frac{\partial N_8}{\partial x} \end{bmatrix} \begin{Bmatrix} u_{x1} \\ u_{y1} \\ u_{z1} \\ u_{x2} \\ \cdots \\ u_{x8} \\ u_{y8} \\ u_{z8} \end{Bmatrix} \tag{A.8}$$

The Jacobian matrix of the element is

$$\mathbf{J} = \begin{bmatrix} \frac{\partial x}{\partial \xi} & \frac{\partial y}{\partial \xi} & \frac{\partial z}{\partial \xi} \\ \frac{\partial x}{\partial \eta} & \frac{\partial y}{\partial \eta} & \frac{\partial z}{\partial \eta} \\ \frac{\partial x}{\partial \mu} & \frac{\partial y}{\partial \mu} & \frac{\partial z}{\partial \mu} \end{bmatrix} \tag{A.9}$$

while the the flexibility matrix of the element for an orthotropic material $\mathbf{D}^{-1}$ can generally be written as

$$\mathbf{D}^{-1} = \begin{bmatrix} \frac{1}{E_x} & \frac{-v_{xy}}{E_x} & \frac{-v_{xz}}{E_x} & 0 & 0 & 0 \\ \frac{-v_{yx}}{E_y} & \frac{1}{E_y} & \frac{-v_{yz}}{E_y} & 0 & 0 & 0 \\ \frac{-v_{zx}}{E_z} & \frac{-v_{zy}}{E_z} & \frac{1}{E_z} & 0 & 0 & 0 \\ 0 & 0 & 0 & \frac{1}{G_{xy}} & 0 & 0 \\ 0 & 0 & 0 & 0 & \frac{1}{G_{yz}} & 0 \\ 0 & 0 & 0 & 0 & 0 & \frac{1}{G_{xz}} \end{bmatrix} \tag{A.10}$$

The assumption of the undeformed FE being a rectangular parallelepiped is hereby adopted. The coordinates $x_1, x_2, x_3, x_4, x_5, x_6, x_7, x_8, y_1, y_2, y_3, y_4, y_5, y_6, y_7, y_8$, and $z_1, z_2, z_3, z_4, z_5, z_6, z_7, z_8$, can then be replaced by L_x, L_y, L_z in the expression of $\mathbf{B}$. The generic expression for $\mathbf{m}$ is thus given as

$$\mathbf{m} = (\rho L_x L_y L_z) \begin{bmatrix}
1/27 & 0 & 0 & 1/54 & 0 & 0 & 1/108 & 0 & 0 & 1/54 & 0 & 0 & 1/54 & 0 & 0 & 1/108 & 0 & 0 & 1/216 & 0 & 0 & 1/108 & 0 & 0 \\
0 & 1/27 & 0 & 0 & 1/54 & 0 & 0 & 1/108 & 0 & 0 & 1/54 & 0 & 0 & 1/54 & 0 & 0 & 1/108 & 0 & 0 & 1/216 & 0 & 0 & 1/108 & 0 \\
0 & 0 & 1/27 & 0 & 0 & 1/54 & 0 & 0 & 1/108 & 0 & 0 & 1/54 & 0 & 0 & 1/54 & 0 & 0 & 1/108 & 0 & 0 & 1/216 & 0 & 0 & 1/108 \\
1/54 & 0 & 0 & 1/27 & 0 & 0 & 1/54 & 0 & 0 & 1/108 & 0 & 0 & 1/108 & 0 & 0 & 1/54 & 0 & 0 & 1/108 & 0 & 0 & 1/216 & 0 & 0 \\
0 & 1/54 & 0 & 0 & 1/27 & 0 & 0 & 1/54 & 0 & 0 & 1/108 & 0 & 0 & 1/108 & 0 & 0 & 1/54 & 0 & 0 & 1/108 & 0 & 0 & 1/216 & 0 \\
0 & 0 & 1/54 & 0 & 0 & 1/27 & 0 & 0 & 1/54 & 0 & 0 & 1/108 & 0 & 0 & 1/108 & 0 & 0 & 1/54 & 0 & 0 & 1/108 & 0 & 0 & 1/216 \\
1/108 & 0 & 0 & 1/54 & 0 & 0 & 1/27 & 0 & 0 & 1/54 & 0 & 0 & 1/216 & 0 & 0 & 1/108 & 0 & 0 & 1/54 & 0 & 0 & 1/108 & 0 & 0 \\
0 & 1/108 & 0 & 0 & 1/54 & 0 & 0 & 1/27 & 0 & 0 & 1/54 & 0 & 0 & 1/216 & 0 & 0 & 1/108 & 0 & 0 & 1/54 & 0 & 0 & 1/108 & 0 \\
0 & 0 & 1/108 & 0 & 0 & 1/54 & 0 & 0 & 1/27 & 0 & 0 & 1/54 & 0 & 0 & 1/216 & 0 & 0 & 1/108 & 0 & 0 & 1/54 & 0 & 0 & 1/108 \\
1/54 & 0 & 0 & 1/108 & 0 & 0 & 1/54 & 0 & 0 & 1/27 & 0 & 0 & 1/108 & 0 & 0 & 1/216 & 0 & 0 & 1/108 & 0 & 0 & 1/54 & 0 & 0 \\
0 & 1/54 & 0 & 0 & 1/108 & 0 & 0 & 1/54 & 0 & 0 & 1/27 & 0 & 0 & 1/108 & 0 & 0 & 1/216 & 0 & 0 & 1/108 & 0 & 0 & 1/54 & 0 \\
0 & 0 & 1/54 & 0 & 0 & 1/108 & 0 & 0 & 1/54 & 0 & 0 & 1/27 & 0 & 0 & 1/108 & 0 & 0 & 1/216 & 0 & 0 & 1/108 & 0 & 0 & 1/54 \\
1/54 & 0 & 0 & 1/108 & 0 & 0 & 1/216 & 0 & 0 & 1/108 & 0 & 0 & 1/27 & 0 & 0 & 1/54 & 0 & 0 & 1/108 & 0 & 0 & 1/54 & 0 & 0 \\
0 & 1/54 & 0 & 0 & 1/108 & 0 & 0 & 1/216 & 0 & 0 & 1/108 & 0 & 0 & 1/27 & 0 & 0 & 1/54 & 0 & 0 & 1/108 & 0 & 0 & 1/54 & 0 \\
0 & 0 & 1/54 & 0 & 0 & 1/108 & 0 & 0 & 1/216 & 0 & 0 & 1/108 & 0 & 0 & 1/27 & 0 & 0 & 1/54 & 0 & 0 & 1/108 & 0 & 0 & 1/54 \\
1/108 & 0 & 0 & 1/54 & 0 & 0 & 1/108 & 0 & 0 & 1/216 & 0 & 0 & 1/54 & 0 & 0 & 1/27 & 0 & 0 & 1/54 & 0 & 0 & 1/108 & 0 & 0 \\
0 & 1/108 & 0 & 0 & 1/54 & 0 & 0 & 1/108 & 0 & 0 & 1/216 & 0 & 0 & 1/54 & 0 & 0 & 1/27 & 0 & 0 & 1/54 & 0 & 0 & 1/108 & 0 \\
0 & 0 & 1/108 & 0 & 0 & 1/54 & 0 & 0 & 1/108 & 0 & 0 & 1/216 & 0 & 0 & 1/54 & 0 & 0 & 1/27 & 0 & 0 & 1/54 & 0 & 0 & 1/108 \\
1/216 & 0 & 0 & 1/108 & 0 & 0 & 1/54 & 0 & 0 & 1/108 & 0 & 0 & 1/108 & 0 & 0 & 1/54 & 0 & 0 & 1/27 & 0 & 0 & 1/54 & 0 & 0 \\
0 & 1/216 & 0 & 0 & 1/108 & 0 & 0 & 1/54 & 0 & 0 & 1/108 & 0 & 0 & 1/108 & 0 & 0 & 1/54 & 0 & 0 & 1/27 & 0 & 0 & 1/54 & 0 \\
0 & 0 & 1/216 & 0 & 0 & 1/108 & 0 & 0 & 1/54 & 0 & 0 & 1/108 & 0 & 0 & 1/108 & 0 & 0 & 1/54 & 0 & 0 & 1/27 & 0 & 0 & 1/54 \\
1/108 & 0 & 0 & 1/216 & 0 & 0 & 1/108 & 0 & 0 & 1/54 & 0 & 0 & 1/54 & 0 & 0 & 1/108 & 0 & 0 & 1/54 & 0 & 0 & 1/27 & 0 & 0 \\
0 & 1/108 & 0 & 0 & 1/216 & 0 & 0 & 1/108 & 0 & 0 & 1/54 & 0 & 0 & 1/54 & 0 & 0 & 1/108 & 0 & 0 & 1/54 & 0 & 0 & 1/27 & 0 \\
0 & 0 & 1/108 & 0 & 0 & 1/216 & 0 & 0 & 1/108 & 0 & 0 & 1/54 & 0 & 0 & 1/54 & 0 & 0 & 1/108 & 0 & 0 & 1/54 & 0 & 0 & 1/27
\end{bmatrix}$$

$$\text{(A.11)}$$

a very similar expression is true for $\mathbf{c}$, while the symbolic generic expression of $\mathbf{k}$ can be derived exactly in the same way but is hereby intentionally omitted for the sake of brevity.

The generic sensitivity expressions $\dfrac{\partial \mathbf{k}}{\partial \beta_i}$, $\dfrac{\partial \mathbf{c}}{\partial \beta_i}$, $\dfrac{\partial \mathbf{m}}{\partial \beta_i}$ as well as $\dfrac{\partial^2 \mathbf{k}}{\partial \beta_j \partial \beta_i}$, $\dfrac{\partial^2 \mathbf{c}}{\partial \beta_j \partial \beta_i}$, $\dfrac{\partial^2 \mathbf{m}}{\partial \beta_j \partial \beta_i}$ with β_i, β_j being design parameters can therefore be calculated as a function of $E_x, E_y, E_z, v_{xy}, v_{xz}, v_{yz}, G_{xy}, G_{xz}, G_{yz}, L_x, L_y, L_z$ by differentiating over the generic expressions for $\mathbf{k}, \mathbf{c}, \mathbf{m}$.

Appendix B. Calculation of the Sound Transmission Loss (STL) of a panel by an SEA approach

In this Appendix, the analysis presented in [11] on the derivation of an expression for the total acoustic transmission coefficient τ of a panel in a wave context is summarized. Considering each wave type $w = w_1, w_2...w_n$ propagating within the composite panel as a separate SEA subsystem we have

$$
\begin{aligned}
P_{12} &= \sum_{w=w_1}^{w_n} P_{12,w} \\
P_{23} &= \sum_{w=w_1}^{w_n} P_{23,w}
\end{aligned}
\tag{B.1}
$$

where P_{12} and P_{23} stand for the power flow between the two rooms and the panel.

The STL is defined as:

$$\text{STL} = 10 \log_{10}\left(\frac{1}{\tau}\right) \tag{B.2}$$

where τ is the transmission coefficient defined as the ratio between the transmitted and the incident sound powers. It can be written as the sum of the resonant and the non-resonant transmission coefficient:

$$\tau = \frac{P_{23} + P_{13}}{P_{inc}} = \sum_{w=w_1}^{w_n} \frac{P_{23,w}}{P_{inc}} + \frac{P_{13}}{P_{inc}} \tag{B.3}$$

where P_{inc} stands for the acoustic power incident on the layered panel, which for a reverberant sound field can be written as:

$$P_{inc} = \frac{\langle p_1^2 \rangle A}{4\rho c} \tag{B.4}$$

where $\langle p_1^2 \rangle$ the mean-square sound pressure. An attempt to calculate the resonant coefficient for each wave type w is hereby made. Assuming a linear system with no energy exchanges between different wave types within the structure, the energy balance of a structural wave subsystem can be written as

$$P_{12,w} = P_{2d,w} + P_{23,w} \tag{B.5}$$

The power dissipated can be written as

$$P_{2d,w} = E_{2,w}\omega\eta_{2,w} \tag{B.6}$$

with $E_{2,w}$ and $\eta_{2,w}$ the vibrational energy and the structural loss factor of wave type w respectively. The vibrational energy of the panel due to wave type w can be written as:

$$E_{2,w} = \rho_s A \langle v_w^2 \rangle \tag{B.7}$$

where ρ_s is the mass per unit area, A is the total area of the panel and $\langle v_w^2 \rangle$ is the mean-square velocity in the panel due to wave type w.

The power flow $P_{12,w}$ can be written using the SEA reciprocity rule, as

$$P_{12,w} = \omega\eta_{12,w}n_1\left(\frac{E_1}{n_1} - \frac{E_{2,w}}{n_{2,w}}\right) = \omega\eta_{21,w}n_{2,w}\left(\frac{E_1}{n_1} - \frac{E_{2,w}}{n_{2,w}}\right) \tag{B.8}$$

where $n_1, n_{2,w}$ are the modal density of the source room and of the wave type w respectively and $\eta_{21,w}$ the coupling loss factor between the receiving room and the wave type w which can be written as:

$$\eta_{21,w} = \eta_{23,w} = \frac{\rho c \sigma_{rad,w}}{\rho_s \omega} \tag{B.9}$$

with ρ the acoustic medium density of the room. The total acoustic energy of the source room can be written as

$$E_1 = \frac{\langle p_1^2 \rangle V}{\rho c^2} \tag{B.10}$$

26

An accurate approximation for the modal density of the source room is expressed as

$$n_1 = \frac{V_1 \omega^2}{2\pi^2 c^3} \tag{B.11}$$

then the modal energy of the source room is

$$\frac{E_1}{n_1} = \frac{2\pi^2 c \left\langle p_1^2 \right\rangle}{\rho \omega^2} \tag{B.12}$$

Using the SEA reciprocity rule again, the power flow from the composite panel to the receiving room can be written as:

$$P_{23,w} = \omega \eta_{23,w} n_{2,w} \left(\frac{E_{2,w}}{n_{2,w}} - \frac{E_3}{n_3} \right) = \omega \eta_{23,w} \left(E_{2,w} - \frac{E_3 n_{2,w}}{n_3} \right) \tag{B.13}$$

It is hereby assumed that $n_3 \gg n_{2,w}$ (reasonable for typically sized cavities and especially for medium and high frequencies) and it is also logical that $E_{2,w} > E_3$, therefore presuming that $E_{2,w} \gg \frac{E_3 n_{2,w}}{n_3}$, Eq.B.13 can be written as

$$P_{23,w} = E_{2,w} \omega \eta_{23,w} \tag{B.14}$$

Eventually, after manipulating Eq.B.4 and Eq.B.6-B.14 and substituting them into Eq.B.5 we get:

$$\frac{\left\langle v_w^2 \right\rangle}{\left\langle p_1^2 \right\rangle} = \frac{2\pi c^2 \sigma_{rad,w} n_{2,w}}{\rho_s \omega^2 A (\rho_s \omega \eta_{2,w} + 2\rho c \sigma_{rad,w})} \tag{B.15}$$

Using Eq.B.4,B.7,B.9,B.14,B.15 and substituting them into Eq.B.3 we get

$$\tau_w = \frac{8\rho^2 c^4 \pi \sigma_{rad,w}^2 n_{2,w}}{\rho_s \omega^2 A (\rho_s \omega \eta_{2,w} + 2\rho c \sigma_{rad,w})} \tag{B.16}$$

which is the expression of the resonant transmission coefficient for wave type w.

List of Figures

Figure 1: Caption of a FE modelled composite layered panel

Figure 2: A schematic representation of the SEA power exchanges and energies for the modelled system.
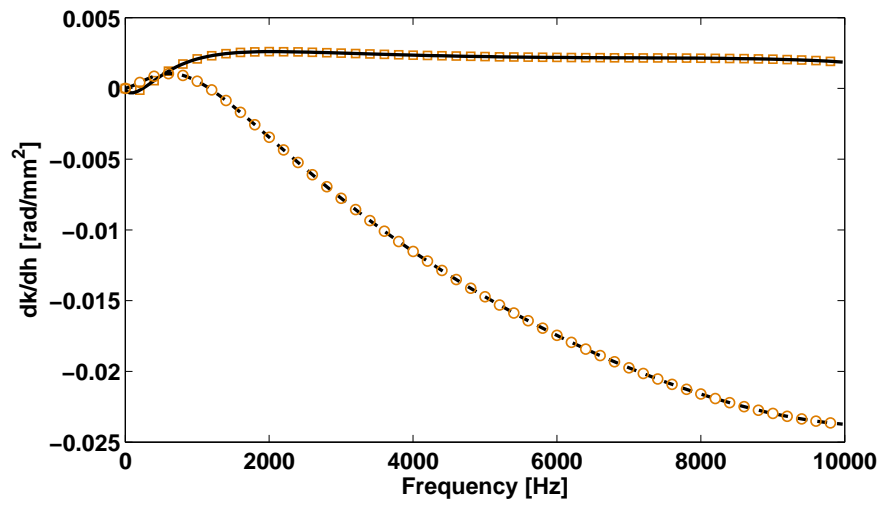
Figure 3: Sensitivity of the propagating wavenumber k under a perturbation of the thickness of the sandwich facesheets for the first flexural wave type of the layered structure: Presented approach for h_1 (−), FD computation for h_1 ($\square$), Presented approach for h_3 (−−), FD computation for h_3 (∘)
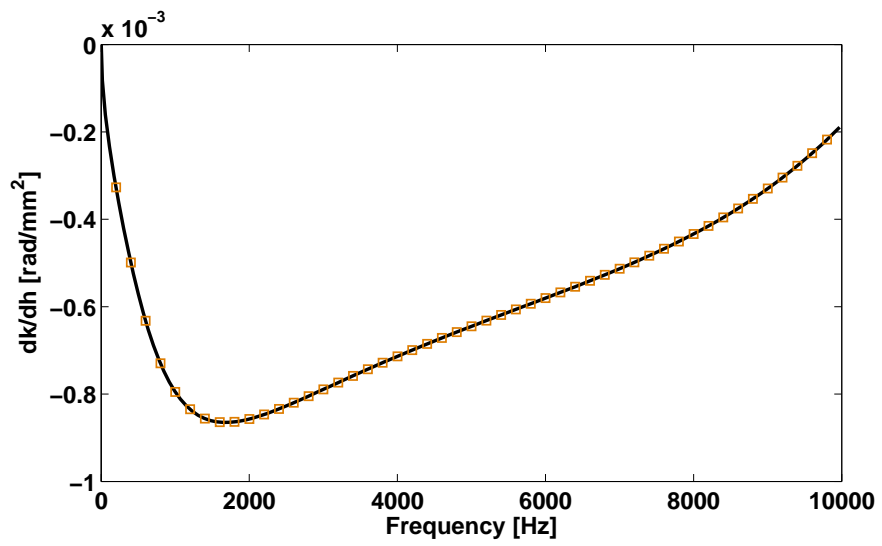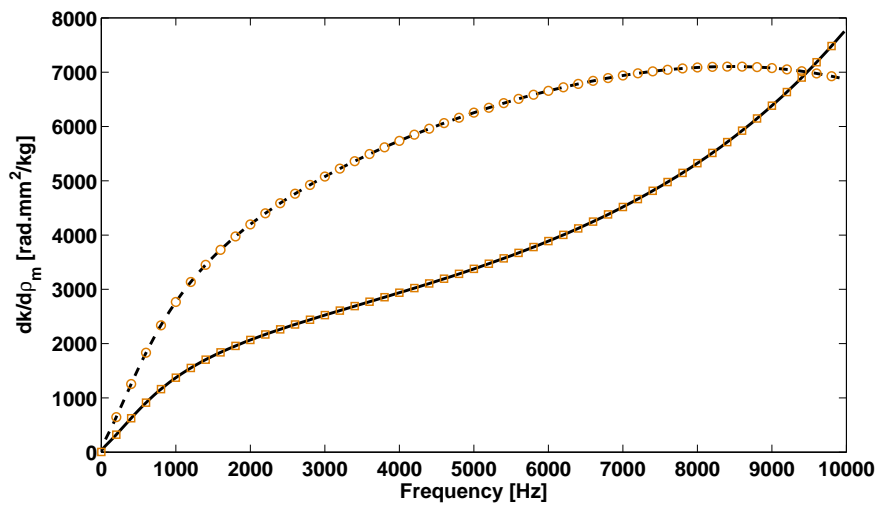
Figure 4: Sensitivity of the propagating wavenumber k under a perturbation of h_2 for the first flexural wave type of the layered structure: Presented approach ($-$), FD computation ($\square$)
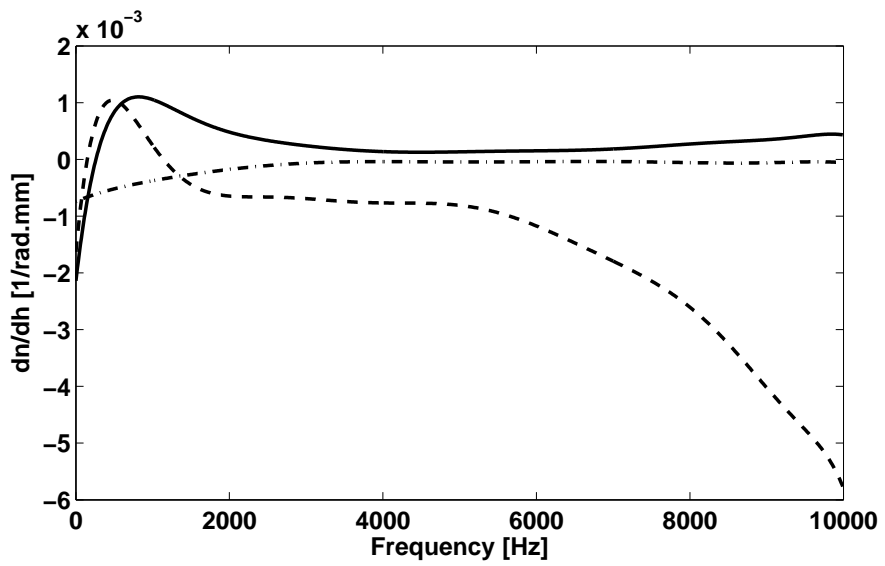
Figure 5: Sensitivity of the propagating wavenumber k under a perturbation of the mass density of the sandwich facesheets for the first flexural wave type: Presented approach for $\rho_{m,1}$ (−), FD computation for $\rho_{m,1}$ (□), Presented approach for $\rho_{m,3}$ (−−), FD computation for $\rho_{m,3}$ (○)
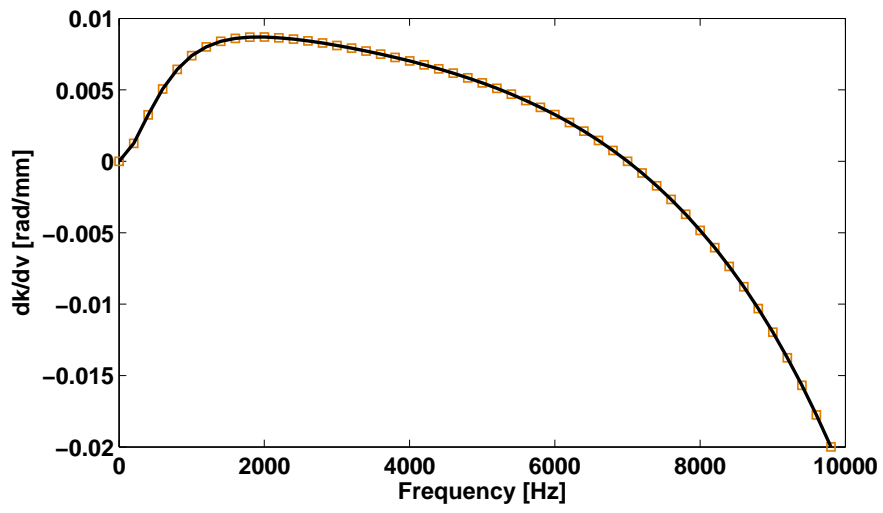
Figure 6: Sensitivity of the propagating wavenumber k under a perturbation of v_2 for the first flexural wave type of the layered structure: Presented approach ($-$), FD computation ($\square$)

Figure 7: Sensitivity of the modal density n of the first flexural propagating wave with respect to the layer thicknesses: with respect to the thickness of the lower facesheet h_1 ($-$), with respect to the thickness of the upper facesheet h_3 ($--$), with respect to the thickness of the core h_2 ($- \cdot -$)
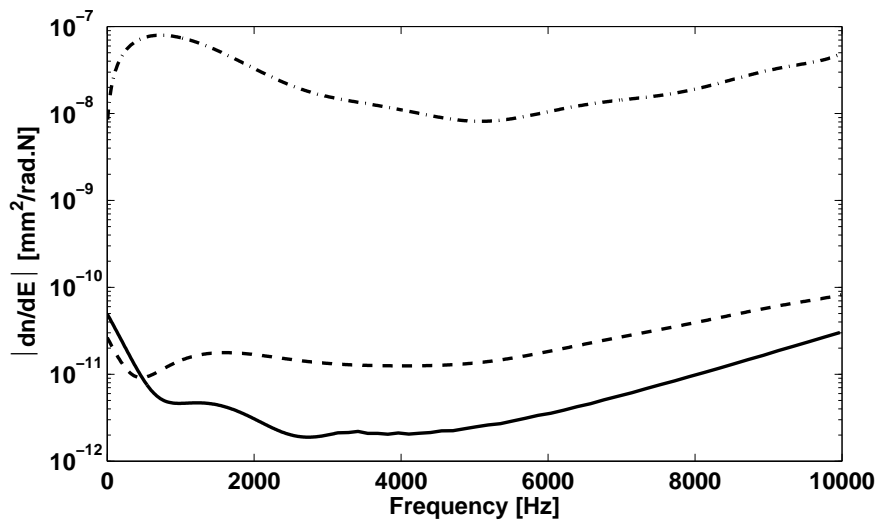
Figure 8: Absolute values for the sensitivity of the modal density n of the first flexural propagating wave with respect to the layer Young's modulus: with respect to the one of the lower facesheet E_1 (−), with respect to the one of the upper facesheet E_3 (−−), with respect to the one of the core E_2 (− · −)
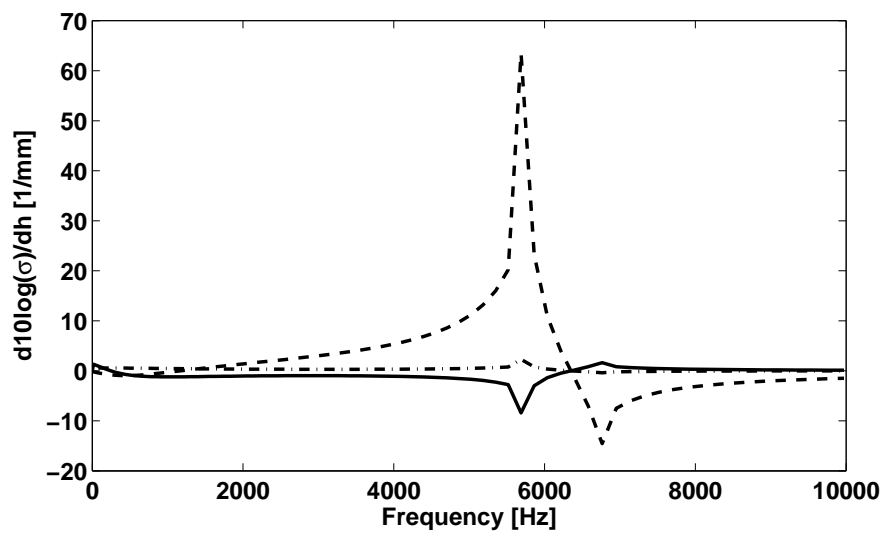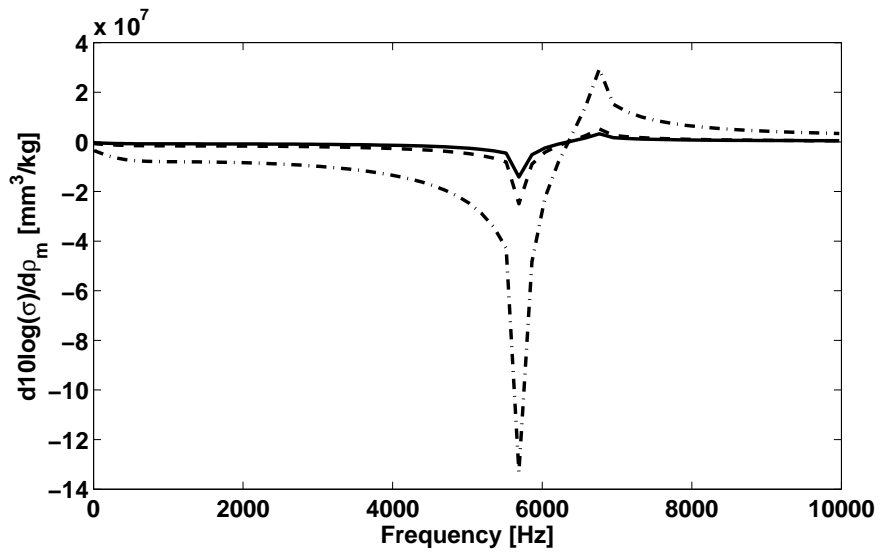
Figure 9: Sensitivity of the logarithmic acoustic radiation efficiency ($10\log(\sigma)$) of the first flexural propagating wave with respect to the layer thicknesses: with respect to the thickness of the lower facesheet h_1 ($-$), with respect to the thickness of the upper facesheet h_3 ($--$), with respect to the thickness of the core h_2 ($- \cdot -$)

Figure 10: Sensitivity of the logarithmic acoustic radiation efficiency ($10\log(\sigma)$) of the first flexural propagating wave with respect to the mass density of the lower facesheet $\rho_{m,1}$ (−), with respect to the density of the upper facesheet $\rho_{m,3}$ (−−), with respect to the density of the core $\rho_{m,2}$ (− · −)
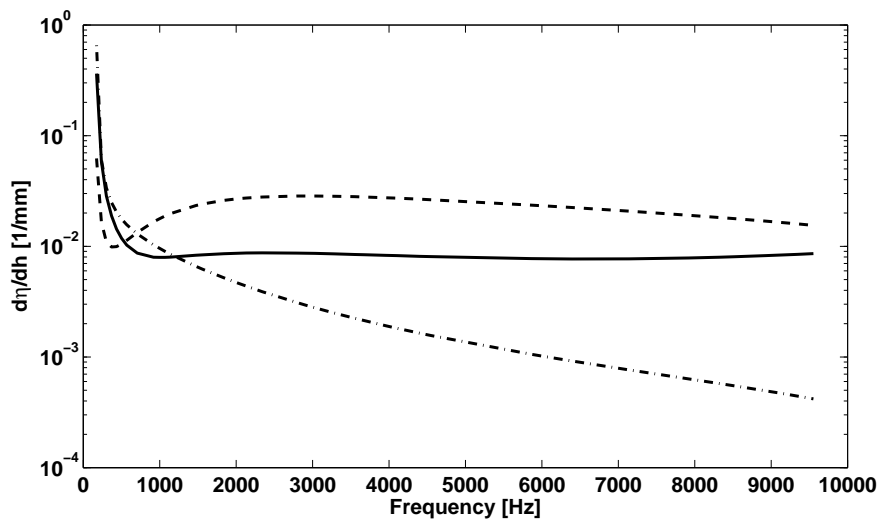
Figure 11: Sensitivity of the total loss factor η of the panel for the first propagating flexural wave with respect to the layer thicknesses: with respect to the thickness of the lower facesheet h_1 (−), with respect to the thickness of the upper facesheet h_3 (−−), with respect to the thickness of the core h_2 (− · −)
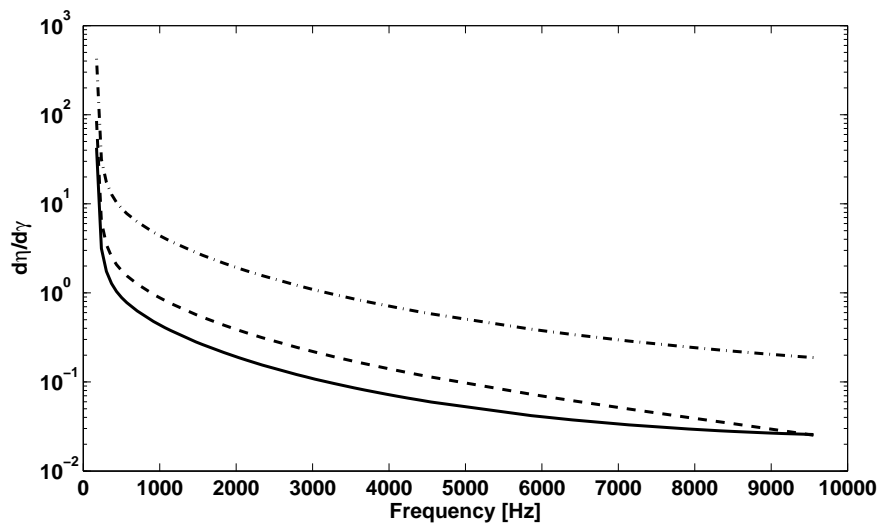
Figure 12: Sensitivity of the total loss factor η of the panel for the first propagating flexural wave with respect to the layer damping coefficient γ: with respect to γ_1 (—), with respect to γ_3 (– –), with respect to γ_2 (– · –)
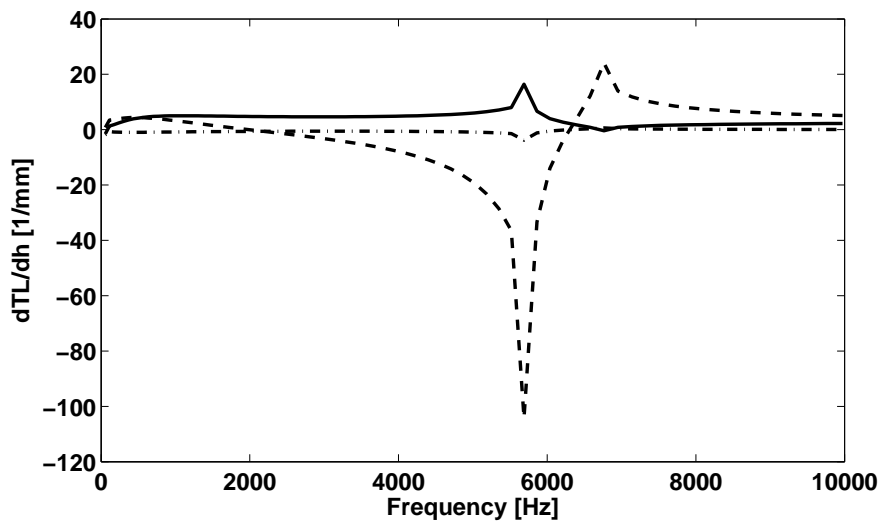
Figure 13: Sensitivity of the sound TL with respect to the layer thicknesses: with respect to the thickness of the lower facesheet h_1 ($-$), with respect to the thickness of the upper facesheet h_3 ($--$), with respect to the thickness of the core h_2 ($-\cdot-$)
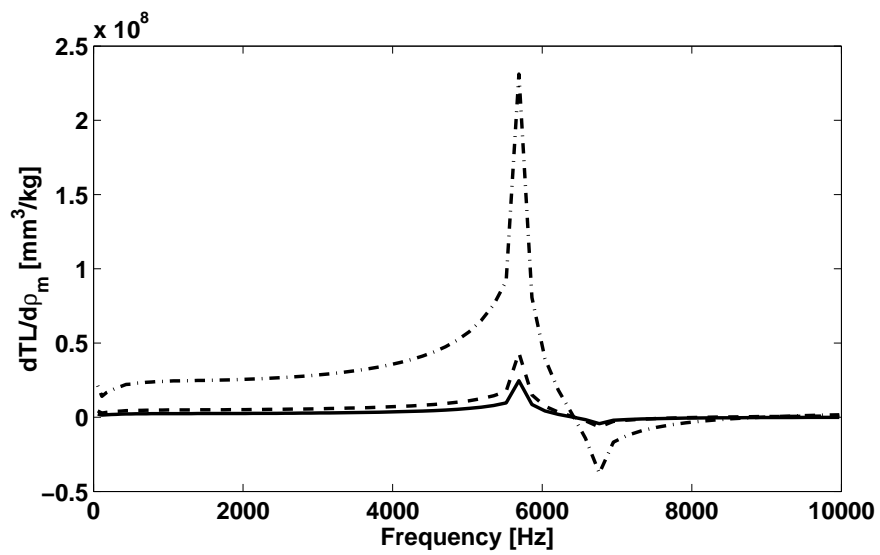
Figure 14: Sensitivity of the sound TL with respect to the layer mass densities: with respect to the density of the lower facesheet $\rho_{m,1}$ (−), with respect to the density of the upper facesheet $\rho_{m,3}$ (−−), with respect to the density of the core $\rho_{m,2}$ (− · −)
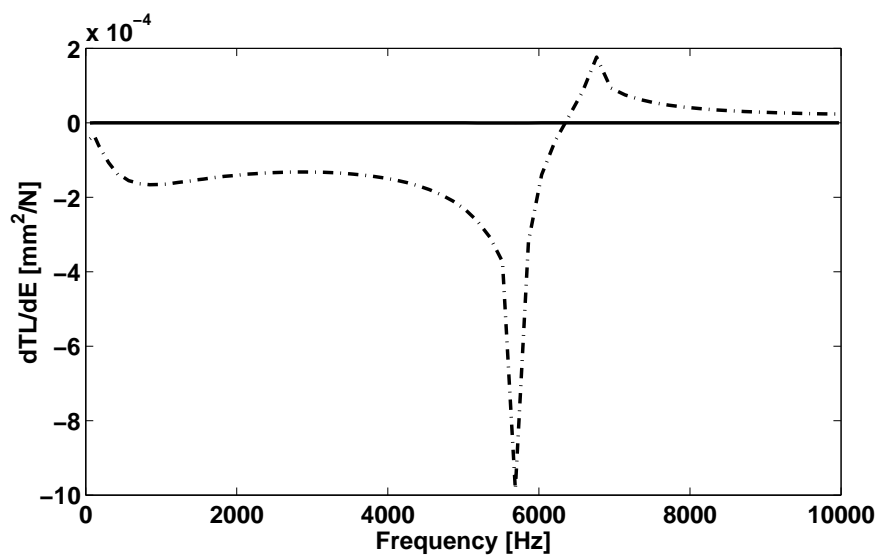
Figure 15: Sensitivity of the sound TL with respect to the layer Young's modulus: with respect to the one of the lower facesheet E_1 $(-)$, with respect to the one of the upper facesheet E_3 $(--)$, with respect to the one of the core E_2 $(-\cdot-)$
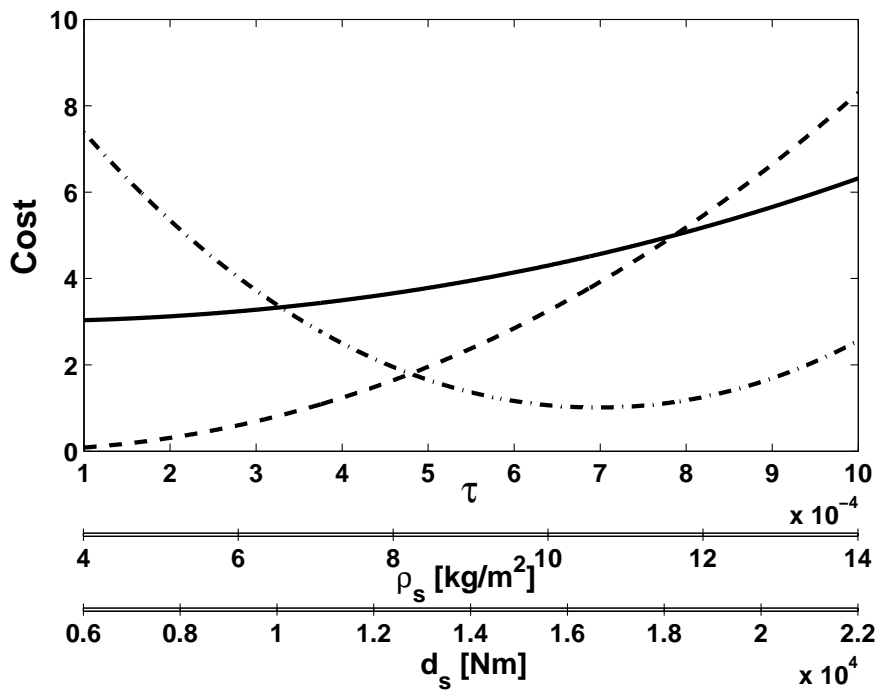
Figure 16: Representation of the cost functions employed within the current optimization process. Cost function corresponding to: The acoustic transmission coefficient τ (−), The surface mass density ρ_s (−−), The flexural stiffness d_s of the panel (− · −)
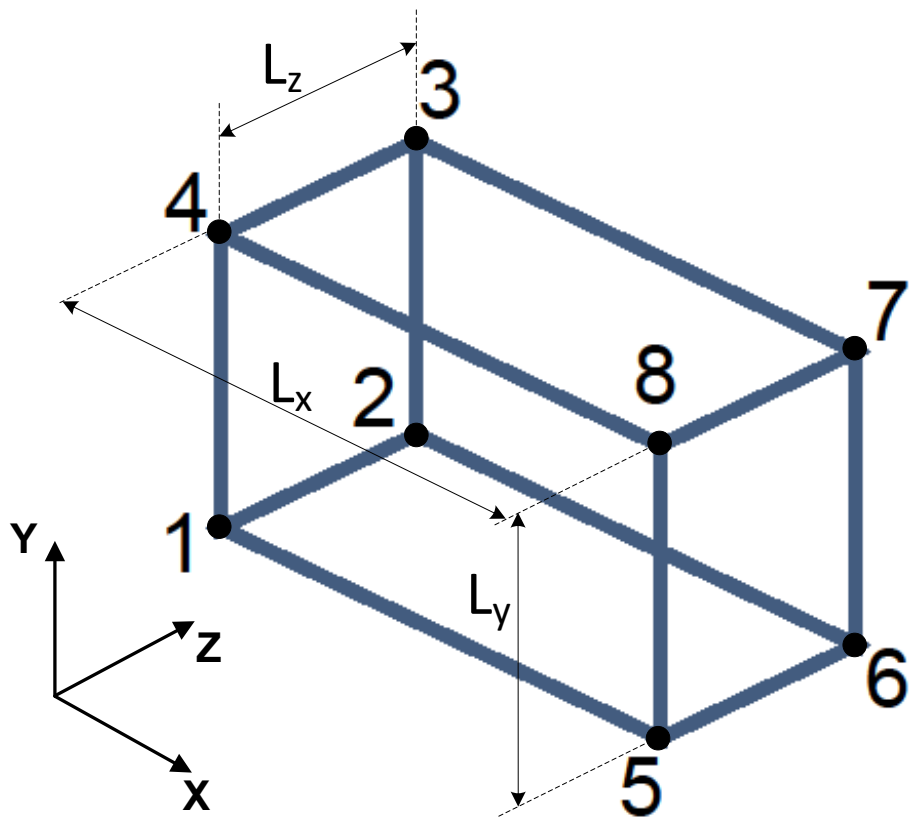
44

Figure 17: The considered solid FE

List of Tables

List of symbols

$\mathbb{M}$, $\mathbb{C}$ and $\mathbb{K}$	Mass, damping and stiffness matrices of the periodic structural segment
$\mathbf{R}$	Transformation matrix
$\mathbf{p}$	Design parameter vector
$\mathbf{q}$	Physical displacement vector
$\mathbf{x}_w$	Right eigenvector corresponding to wave mode w
$\mathcal{F}(\mathbf{p})$	Objective cost function
c	Wave velocity in acoustic medium
L_x, L_y	Dimensions of the composite panel in the x and y directions
k_x, k_y	Wavenumbers in the x and y directions
k_w	Wavenumber corresponding to wave mode w
$c_{g,w}$	Group velocity of wave mode w
n_w	Modal density of wave mode w
d_s	Static flexural stiffness of the structural panel
A	Surface of the structural panel
$E_{x,l}$, $E_{y,l}$ $E_{z,l}$	Young's moduli of layer l
$v_{xy,l}$ $v_{xz,l}$ $v_{yz,l}$	Poisson's ratios of layer l
$G_{xy,l}$ $G_{xz,l}$ $G_{yz,l}$	Shear moduli of layer l
h_l	Thickness of layer l
β_i, β_j	Design parameters
γ_l	Damping coefficient of layer l
ε_x, ε_y	Propagation constants in the x and y directions
η_w	Global damping loss factor of the panel under the passage of wave mode w
κ	Acoustic wavenumber
λ_w	Eigenvalue corresponding to wave mode w
ξ_i, δ_i, ζ_i	Design cost coefficients
ρ	Acoustic medium density
$\rho_{m,l}$	Mass density of layer l
ρ_s	Mass per unit area of the structural panel
$\sigma_{rad,w}$	Radiation efficiency of wave mode w
τ_w	Resonant acoustic transmission coefficient of wave mode w
τ_{nr}	Non resonant acoustic transmission coefficient
ϕ	Considered direction of propagation
ω	Angular frequency
ω_w	Angular frequency at which a certain wave mode w occurs with predefined ε_x, ε_y